SUMO4 regulates DNA double-strand break repair independently of conjugation

Alexander J. Garvin[1], Alexander J. Lanz[1], Ruth M. Densham[1], Joanna R. Morris[1]

1: Birmingham Centre for Genome Biology and Institute of Cancer and Genomic Sciences, College of Medical and Dental Schools, University of Birmingham, B15 2TT, UK.

Correspondence: j.morris.3@bham.ac.uk, a.j.garvin@bham.ac.uk

Keywords: SUMO, SUMO4, DNA repair, Homologous Recombination, RAP80, SENP1.

Abstract

The small ubiquitin-like modifier (SUMO) family is composed of five members, SUMO1, the highly similar SUMO2/SUMO3, SUMO4 and the tissue-specific SUMO5 (*SUMO1P1*). Sequence variation in SUMO4 is thought to prevent its maturation, resulting in an un-conjugatable SUMO isoform, and consequently, its functions are poorly understood. Here we show for the first time that SUMO4 promotes DNA double-strand break signalling in a manner distinct from SUMO1 or SUMO2/3. We show that SUMO4 function depends on interaction with partner proteins through SUMO interacting motifs and, on its inability, to be conjugated. We show that SUMO4 promotes the activity of the SUMO protease SENP1. In the absence of SUMO4, reduced SENP1 catalytic activity results in hyperSUMOylation that unbalances the recruitment of several DSB repair factors, including RAP80. These data reveal that SUMO4 acts as a buffer for the SUMOylation system.

Introduction

The repair of DNA double-strand breaks (DSBs) is dependent on a series of tightly regulated post-translational modifications (PTMs) of both the surrounding chromatin environment and the repair factors themselves (Dantuma and van Attikum, 2016). PTMs, including phosphorylation, acetylation, ubiquitination and SUMOylation tune the DSB repair machinery to ensure correct pathway choice and amplitude of response, collectively ensuring genomic stability (Garvin, 2019).

Conjugation of SUMO (Small Ubiquitin-like Modifiers) to target lysine (SUMOylation) has essential roles in the repair of DNA double-strand breaks through regulating recruitment, activity and clearance of proteins localising to DSBs (Galanty et al., 2009, Hariharasudhan et al., 2022, Morris et al., 2009, Galanty et al., 2012, Luo et al., 2012, Pfeiffer et al., 2017, Vyas et al., 2013, Yin et al., 2012, Garvin et al., 2019). Many proteins involved in DSB repair signalling are SUMOylated in basal and stressed conditions, but for many, the role modifications have is not clear (Garvin and Morris, 2017, Hendriks and Vertegaal, 2016, Kumar et al., 2017). Multiple DSB repair factors interact with SUMO1-3 through SUMO Interacting Motifs (SIMs) (Pfeiffer et al., 2017, Guzzo et al., 2012, Hu et al., 2012) or other SUMO binding domains such as ZZ domain (Danielsen et al., 2012), or MYM type zinc fingers (Guzzo et al., 2014, Lee et al., 2022). These interactions are consistent with the proposed role

of SUMO as a “molecular glue” wherein high local concentrations of SUMOylated factors - such as chromatin surrounding a DSB, act as binding platforms (Psakhye and Jentsch, 2012, Gonzalez-Prieto et al., 2021). Disruption of the balance of conjugation and deconjugation has profound effects on a cell's ability to repair DSBs and maintain genomic stability (Garvin, 2019, Garvin et al., 2013, Dou et al., 2010, Dhingra and Zhao, 2019, Schick et al., 2022).

The SUMO family is composed of five members, SUMO1, the highly similar SUMO2 and SUMO3 (SUMO2/3), SUMO4 and SUMO5 (SUMO1P1). All conjugated isoforms utilise the same E1-E2-E3 conjugation enzyme machinery. Paralogue specific modification can have different outcomes for the modified protein due to discrimination by protein “readers” of SUMO modification between isoforms (Varejao et al., 2020, Pichler et al., 2017, Lascorz et al., 2021).

SUMO4 is a protein-coding retrogene located within an intron of the *TAB2* gene that shares 86% homology with SUMO2. SUMO4’s conjugation status is controversial. Some reports suggest SUMO4 is conjugated under certain conditions (Guo et al., 2005, Wei et al., 2008, Garvin et al., 2022). However, proline 90 within the C terminal tail interferes with SUMO protease-mediated exposure of the di-glycine motif, so P90 is expected to render SUMO4 un-conjugatable. Little is known about the biochemical or physiological activity of the SUMO4 protein.

Here we describe a critical role for unconjugated SUMO4 in DSB signalling. We show two surfaces are required for SUMO4 function: its SIM binding groove and the region surrounding Met55. We find SUMO4 regulates the catalytic activity of the SUMO protease SENP1, which in turn regulates SUMO1-3 conjugate amplitude. In DSB signalling SUMO4 regulated SENP1 catalytic activity restricts the accumulation of the RAP80, maintaining a correct balance of DSB repair factors. This work reveals that SUMO4 is a key regulator of the SUMO system.

SUMO4 is required for DSB repair

SUMO1 and SUMO2/3 isoforms have non-redundant roles in DSB repair, although the exact roles for the two pathways are not fully understood (Garvin and Morris, 2017). To determine if SUMO4 has a role, we used siRNA targeting SUMO4 but not the closely related SUMO2 or SUMO3 (Figure 1a). All tested SUMO4 antibodies cross-react with SUMO2/3 (Garvin et al., 2022), but we confirmed knockdown of exogenous 6xHis-HA SUMO4 with our siRNA sequences (Supplemental Figure 1a). Using integrated *SceI* reporters of HR (gene conversion) and NHEJ repair, we assessed the influence of siRNA to each SUMO family member. For both repair pathways, we found siRNA to SUMO4 reduced GFP repair outcome (Figure 1b-c). We next measured the kinetics of γH2AX foci following exposure to 4 Gy ionising irradiation (IR) in U2OS treated with siRNAs to each isoform. All, including SUMO4 siRNA slowed the clearance of γH2AX foci in both EdU negative and positive cells (Figure 1d and Supplemental Figure 1b).

Next, we sought to determine what influence SUMO4 depletion has on DSB signalling. We first assessed MDC1, a well-characterised repair factor that requires SUMOylation for clearance from DSBs (Luo et al., 2012, Pfeiffer et al., 2017, Garvin et al., 2019, Galanty et al., 2012, Yin et al., 2012). Consistent with the literature, depletion of either SUMO1 or SUMO2/3

slowed MDC1 foci resolution, while SUMO4 had no effect (Figure 1e and Supplemental Figure 1c).

We assessed the kinetics of RNF168 and found reduced foci accrual in SUMO1 and SUMO4 depleted cells, while SUMO2/3 depletion resulted in excessive RNF168 accrual at early time points (Figure 1f and Supplemental Figure 1d). 53BP1 is recruited to damaged chromatin by ubiquitinated H2A/H2AX generated by RNF168 (Fradet-Turcotte et al., 2013). We found siSUMO1 ablated 53BP1 foci accumulation while SUMO2/3 had less effect (Figure 1g and Supplemental Figure 1e). This is consistent with earlier reports that propose this aspect of DSB repair is primarily SUMO1 dependent (Galanty et al., 2009, Morris et al., 2009, Danielsen et al., 2012). SUMO4 siRNA depletion had similar effects on 53BP1 foci kinetics to siSUMO1. We examined end-resection and homologous recombination as measured by RPA32 pSer33 foci and RAD51 foci, respectively and found that depletion of SUMO4 caused a reduction in both these measures (Figure 1h-i).

To compare SUMO isoforms, we tested colony survival of SUMO isoform depleted U2OS cells following treatments with IR, camptothecin, cisplatin or the PARP1/2 inhibitor, olaparib. SUMO4 depletion increased sensitivity to these agents to a level comparable to, or greater than, SUMO1-3 depletion (Figure 1j-m). SUMO4 siRNA depletion also sensitised HeLa cells to IR, camptothecin and cisplatin (Supplemental Figure 1f). To further explore the role of SUMO4, we used CRISPR-Cas9 to target the *SUMO4* locus in U2OS cells, generating clones that lacked SUMO4 expression, hereafter SUMO4^{KO}. Independent U2OS-SUMO4^{KO} clones generated from different gRNAs, were similarly sensitive to treatments with IR, CPT, and cisplatin (Figure 1n and Supplemental Figure 1g-h). Taken together, these data indicate that SUMO4 promotes the cellular response to DNA damage.

Conjugation independent role of SUMO4 in DSB repair

To address the required conjugation status of SUMO4, we performed complementation analysis using Wild-type (WT) protein, SUMO4 bearing a stop codon prior to the glycine residues essential for conjugation in other isoforms (T91X) and SUMO4 bearing a stop codon after the glycine residues (V94X), thereby artificially maturing it, and making SUMO4 conjugation proficient (Figure 2a). In line with expectations, we noted that the subcellular localisation of the conjugation proficient mutant V94X-SUMO4 was nuclear, like SUMO2/3, while T91X-SUMO4 showed cytoplasmic and nuclear localisation resembling the WT protein (Supplemental Figure 2a). We tested each mutant in complementation assays on both an siRNA depleted and SUMO4^{KO} background using 53BP1 and RAD51 as markers of DSB signalling. SUMO4 lacking the di-glycine residues, T91X-SUMO4, was able to restore each of these markers to control/WT levels in both backgrounds, while the conjugation-proficient V94X-SUMO4, was defective (Figure 2b-c and Supplemental Figure 2b-c). Consistent with these findings, colony survival analysis of complemented cells showed the conjugation deficient T91X-SUMO4 and WT-SUMO4, but not the conjugation proficient mutant, were able to restore resistance to IR, CPT, cisplatin and olaparib (Figure 2d-e and Supplemental Figure 2d-i). V94X-SUMO4 was also unable to restore GFP reporter activity in either HR or NHEJ assays (Figure 2f). Collectively these results suggest conjugation is deleterious for SUMO4 function and that the inability to conjugate is required in DSB repair.

SUMO4 requires its SIM binding and Met55 patch for DSB repair activity

SUMO4 shares several features with its SUMO2 ancestor, including the groove that partner proteins bearing a SUMO interacting motifs (SIMs) bind to (Figure 3a). To determine if this feature is functionally conserved, we generated mutations analogous to the well-characterised mutations in SUMO2, SUMO4 QFI-A (Q31A/F32A/I34A) (Merrill et al., 2010). We also assessed the common SUMO4 polymorphism M55V (rs237025) due to its conservation across SUMO family members and its surface exposure (Figure 3a-b). Neither mutation impacted SUMO4 localisation (Supplemental Figure 2a). SUMO4 siRNA depleted cells complemented with SUMO4 QFI-A or M55V were defective in 53BP1 and RAD51 foci formation, showed poor HR repair in *SceI* assays, and were sensitive to DSB inducing agents (Figure 3c-g), as were similarly complemented SUMO^{KO} cells (Supplemental Figure 3a-f). To test whether M55 of SUMO4 might be part of a wider required region of the SUMO4 surface, we mutated two residues proximal and distal to M55 and complemented SUMO4^{KO} cells (Supplemental Figure 3g). Except for Q57A, each of these mutants also failed to restore IR, cisplatin or olaparib resistance and did not restore control levels of γH2AX, 53BP1 or RAD51 foci (Supplemental Figure 3h-k). These data suggest that the SIM and M55 patches of SUMO4 have important roles in DSB repair.

SUMO4 maintains SUMO homeostasis in response to genotoxic stress

To identify interactors of SUMO4, we performed immunoprecipitations followed by LC MS/MS using WT, QFI-A -mutant and M55V-mutant SUMO4 proteins from untreated and irradiated HEK293 cells. This analysis identified several proteins in WT-SUMO4 and M55V-SUMO4 precipitates that were absent in the QFI-A precipitates, including characterised SUMO interactors PML, PIAS1, ZMYM2, BLM and SIMC1 (Figure 4a). Indeed, the identified SUMO4 interactors overlap with other SUMO interactomes (Figure 4a-b) (Gonzalez-Prieto et al., 2021, Shire et al., 2016, Bruninghoff et al., 2020). These data suggest SUMO4 associates with the SUMO system. M55V-SUMO4 and WT-SUMO4 had both shared and distinct interactions suggesting a subset of interactors depend on the M55 patch. Interactors unique to WT SUMO4 and dependent on both SIM and M55 patches were rare, suggesting few are dependent on both surfaces, consistent with their spatial distance from one another (Figure 4b and Figure 3b).

The observation that several SUMO conjugation/deconjugation components interact with SUMO4 (Figure 4b) lead us to examine its impact on SUMO1-3 conjugates. In IR-treated SUMO4^{KO} or SUMO4 siRNA-treated cells, we observed increased SUMO1 and SUMO2/3 conjugates and immunofluorescence intensity (Figure 5a-c, Supplemental Figure 4a). Intriguingly, these measures were suppressed by the expression of WT-SUMO4, but not of the QFI-A or M55V mutants (Figure 4d-e).

PML was the most enriched interactor of WT SUMO4 and showed reduced immunoprecipitation with the SUMO4 QFI-A mutant (Figure 4b). We noted an increase in the number of PML-NBs in cells lacking SUMO4 (Figure 5f-g). However, in contrast to the impact on global SUMO conjugates, complementation with M55V-SUMO4, or with the variants of the M55 patch, restored PML-NBs to the number seen in cells complemented with WT-SUMO4 (Figure 5h, Supplemental Figure 4b). The PML-NB component, Sp100, showed similar

sensitivity to SUMO4 depletion and restoration (Figure 5i). Thus, while SUMO4 influences PML-NBs, this impact is, at least in part, separate from the impact of SUMO4 on DSB repair, which requires the M55-face (Figure 3).

To test if increased SUMOylation observed following SUMO4 loss might relate to reduced repair proficiency, we reduced SUMO conjugation by short treatments with the SUMO E1 inhibitor, ML-792 (He et al., 2017). Remarkably, ML-792 treatment improved 53BP1 and RAD51 foci accrual and cellular resistance to IR in both SUMO4 siRNA-treated and SUMO4^{KO} cells (Figure 5j-m). To challenge this idea further, we tested depletion of the SUMO E2 enzyme UBC9, and found it also improved the accumulation of 53BP1 and RAD51 foci (Figure 5n-p) and IR-resistance of SUMO4^{KO} cells (Supplemental Figure 4c). These data are consistent with the notion that hyperSUMOylation drives defective DSB signalling in the absence of SUMO4.

SUMO4 modulates SUMO protease SENP1 activity

The increase in SUMO conjugates detected on SUMO4 disruption could result from increased SUMOylation or decreased deSUMOylation. The SENP (Sentrin/SUMO specific protease) enzymes rapidly cleave isopeptide bonds between SUMO isoforms and their conjugates, so that cysteine protease inhibition is required to suppress these when examining SUMO-conjugates in cell lysates. By generating lysates without cysteine protease inhibitors, we approximated the rate of SUMO1 and SUMO2/3 conjugate turnover. In SUMO4^{KO} cells, we found both SUMO1 and SUMO2/3 high molecular weight species were more slowly processed compared to the parental U2OS (Figure 6a-d). Turnover kinetics could be restored by the reintroduction of WT-SUMO4 (Figure 6a-d), suggesting SUMO proteases may be less active in SUMO4^{KO} cells.

To explore whether a particular SUMO protease is influenced by SUMO4 we incubated cell lysates with recombinant SUMO1 or SUMO2-Vinyl sulfones. These are active site-directed irreversible inhibitors of SENPs (Kolli et al., 2010), that we reasoned act as a proxy for catalytic activity / catalytic cysteine availability. We measured the labelling of the major SUMO proteases SENP1, SENP3 and SENP6. Of these, we found SENP1 showed reduced labelling in the SUMO4^{KO} lysates (Figure 6e-f and Supplemental 5a-d). We identified SENP1 as a SUMO4 interactor (Figure 4b), and these data suggest SENP1 activity requires SUMO4. Poor SUMO1-VS labelling of SENP1 in the absence of SUMO4 could be improved by WT-SUMO4 expression, but not by expression of the QFI-A or M55V mutants (Figure 6g), correlating with the impact of SUMO4 mutants on the DSB repair response.

We compared the impact of SENP1 and SUMO4 depletion on SUMO2/3 deconjugation rates and found they were similar (Figure 6h) and noted that co-depletion of SUMO4 and SENP1 is epistatic in colony survival assays of cells treated with IR, CPT, cisplatin or olaparib, and in the promotion of DSB repair foci (γH2AX, MDC1, RNF168, 53BP1 and RAD51) (Figure 6i-k Supplemental Figure 5e-i). We found that the catalytic activity of SENP1 is required for the promotion of DNA-damage signalling as complementation of siSENP1 cells with WT, but not the catalytic mutant, C603A-SENP1, restored γH2AX and RAD51 foci levels, and was essential for the survival of cells treated with IR, CPT, cisplatin or olaparib (Figure 6l-o and Supplemental Figure 5k-l). These findings suggest SUMO4-SENP1 function acts to promote the cellular response to DNA damage.

The accumulation of RAP80 at DSBs is regulated by SUMO4-SENP1

RAP80 contains tandem SIM-ubiquitin interaction motifs that interact with both SUMO and K63-Ub (Guzzo et al., 2012, Hu et al., 2012). To determine if RAP80 is affected by SUMO4 loss, we measured RAP80 foci kinetics in siSUMO4 cells. As expected, depletion of either SUMO1 or SUMO2/3 resulted in reduced RAP80 foci accumulation. Conversely, loss of SUMO4 caused a hyperaccumulation of RAP80 foci, which could be reversed by complementation with WT-SUMO4 but not QFI-A- or M55V mutant SUMO4 (Figure 7a &b). Similarly, depletion of siSENP1 resulted in increased RAP80 foci number, which could be complemented by WT-SENP1, but not C603A-SENP1 (Figure 7c). Over-expressing SENP1 reduced RAP80 foci numbers in a catalytic dependent manner (Figure 7d-e). Remarkably siRNA targeting SENP2,3,5,6 or 7 had no impact on RAP80 foci numbers (Figure 7f), suggesting SENP1 specifically antagonises RAP80 accrual. Co-depletion of SENP1 and SUMO4 did not increase RAP80 foci numbers more than either depletion alone, suggesting SUMO4 and SENP1 are epistatic in relation to RAP80 foci number (Figure 7g). These data suggest SUMO4-SENP1 catalytically regulates the accumulation of RAP80 foci.

The hyperaccumulation of RAP80 in SUMO4^{KO} cells was dependent on upstream K63-Ub signalling components RNF8, RNF168 and UBC13 as depletion of these factors in both U2OS and SUMO4^{KO} cells reduced RAP80 foci accrual (Figure 7h). Components of the SUMO conjugation system also contributes to the hyperaccumulation of RAP80 in SUMO4^{KO} cells (Figure 7i). These data suggest that the hyperaccumulation of RAP80 is through the canonical ubiquitin-SUMO recruitment pathway.

RAP80 acts as a recruitment module for the BRCA-A complex, which in turn contains at least two biochemical features that can alter DSB repair response. The first is the de-ubiquitinating enzyme BRCC36 which removes K63-Ub conjugates that promote RNF168 spreading and deposition of the H2A-Ub mark recognised by both 53BP1 and BARD1 (Kakarougkas et al., 2013, Ng et al., 2016, Patterson-Fortin et al., 2010, Shao et al., 2009, Sobhian et al., 2007). The second is Abraxas, which interacts with the BRCT repeats of BRCA1 and sequesters the BRCA1-BARD1 dimer (Coleman and Greenberg, 2011, Cooper et al., 2009). To test whether these activities contribute to defective DSB repair in SUMO4 deficient cells, we overexpressed a catalytic mutant of BRCC36 and a phosphorylation mutant of Abraxas. When overexpressed, the catalytic mutant of BRCC36, H124Q/H126Q (HQ), restored the IR, CPT and olaparib resistance in SUMO4^{KO} cells. The Abraxas phosphorylation mutant S404A/S406A (SA) which is deficient in BRCA1 interaction (Wu et al., 2016), only restored resistance to CPT and olaparib but not IR in SUMO4^{KO} cells (Figure 7j-m). Collectively these data suggest that SUMO4 regulated SENP1 catalytic activity antagonises the formation of RAP80 foci to restrict the excessive accumulation of the K63 deubiquitinase BRCC36 and BRCA1-BARD1 antagonist Abraxas.

Discussion

Here we show a clear function for the SUMO isoform, SUMO4, and unequivocally show its function in DSB repair is tightly related to its non-conjugated status. We also demonstrate that artificially promoting SUMO4 conjugation is deleterious to DSB repair. One potential explanation for this is the presence of Pro90 which both prevents maturation of immature

SUMO and renders SUMO conjugates resistant to SENP enzymes (Bekes et al., 2011, Owerbach et al., 2005). This study supports the notion that SUMO4 is unique within the SUMO family and signals in its free state.

We find that M55V-SUMO4 has overlapping interactors with WT-SUMO4, suggesting M55V modulates a subset of SUMO4 functions rather than eliminates them. Indeed, suppression of PML-NBs is independent of M55 status. Multiple studies indicate SUMO4 M55V predisposes certain populations to diabetes and may predispose individuals to other autoimmune disorders (Guo et al., 2004, Li et al., 2017b, Lin et al., 2007, Noso et al., 2005, Sedimbi et al., 2007, Tong et al., 2021, Tsurumaru et al., 2006, Zhang et al., 2017, Bohren et al., 2004). Our data support the possibility that the M55V polymorphism is functional, but whether the disease states associated with it relate to the phenotypes we describe is unknown.

Our data imply that the SIM-interacting groove and M55 patch of SUMO4 modulate global SUMO dynamics, at least in part via the SUMO protease SENP1. How SUMO4 regulates SENP1 function is not yet clear. We note that we identified SENP1 as a SUMO4-SIM groove dependent interactor and that the SIM binding QFI-A mutant of SUMO4 is defective in restoring SENP1 catalytic activity so that the action of SUMO4 on SENP1 may be direct. It is also possible that SUMO4's structural similarity to SUMO2/3, but its inability to be conjugated, modulates SENP1 catalytic activity indirectly.

We propose that the accumulation of the SUMO-Ubiquitin recognition component of the BRCA-A complex, RAP80, is sensitive to SENP1 catalytic activity. Our data show that SUMO proteases, alongside the deubiquitinating (DUB) enzymes (Wu et al., 2019, Li et al., 2017a, Typas et al., 2016), influence RAP80 dynamics. The role of the BRCA-A complex in DSB repair is not fully understood but the combined contribution of the K63 linkage specific DUB BRCC36 and the BRCA1 interactor Abraxas have important roles in limiting BRCA1 dependent DNA end resection and controlling K63-Ub signalling (Lombardi et al., 2017). We find that over-expressing a catalytic mutant of BRCC36 is sufficient to restore SUMO4^{KO} cell resistance to IR, CPT and olaparib, suggesting the catalytic function of BRCC36 contributes to the repair defect of cells lacking SUMO4. Intriguingly, suppression of the Abraxas-BRCA1 interaction restored SUMO4^{KO} resistance to CPT and olaparib but not IR, consistent with the previously described role of the complex inhibiting DNA resection (Coleman and Greenberg, 2011, Sobhian et al., 2007). We do not discount the potential for indirect influences of altered SENP function, for example, through a combined disrupted SUMO1 and SUMO2/3 signalling.

These findings add to a growing appreciation that different SUMO proteases have distinct functions, giving rise to distinct DSB signalling defects. For example, SENP2, SENP6 or SENP7 disruption respectively cause excessive MDC1 turnover, RPA70-RAD51 interaction defects or chromatin compaction defects (Garvin et al., 2019, Dou et al., 2010, Garvin et al., 2013). Our comparison of SUMO isoforms in the damage response also highlights their divergence showing distinct acute requirements for SUMO1 *Vs* SUMO2/3 and now illustrating that SUMO4 has an entirely separate role where it acts as a buffer for the SUMO-system.

The authors declare no conflict of interest.

Author Contributions. AJG designed the study, undertook all blots, cell work, imaging and analysis, AL generated purified SUMO isoforms, JRM oversaw the study. AJG and JRM co-wrote the paper. All Authors have commented and edited the manuscript.

Acknowledgements Grant funding: Wellcome Trust 206343/Z/17/Z (A.J.G), University of Birmingham (A.L). We thank the Microscopy and Imaging Services at Birmingham University (MISBU) in the Tech Hub facility for microscope support and maintenance. We thank Jeremy Stark (City of Hope, Duarte U.S.A.) for U2OS DR-GFP and NHEJ-EJ5 cells

Methods

Cell culture and stable cell lines, and SUMO4^{KO}, colony assays, survival assays, reporter assays.

All cell lines were cultured in DMEM supplemented with 10% FBS and 1% Penicillin-Streptomycin. FlpIn stable cell lines were generated using U2OS$^{TrEx\text{-}FlpIn}$ (a gift from Grant Stewart, University of Birmingham) cells transfected with pcDNA5/FRT/TO based vectors (Supplementary Table 2) and the recombinase pOG44 (Invitrogen) using FuGene6 (Promega) at a ratio of 4 μl FuGENE/ 1 μg DNA. After 48 hr, cells were grown in hygromycin selection media (100 μg/ml) until colonies formed on plasmid-transfected plates but not controls. SUMO4 knockout U2OS$^{TrEx\text{-}FlpIn}$ were generated using two different guide RNAs pSpCas9 (BB)-2A PURO (GenScript) plasmids that target the SUMO4 gene at nucleotides (relative to start codon) 150-171 (gRNA #1) and 186-204 (gRNA #4). For each gRNA three 10 cm^2 plate of U2OS$^{TrEx\text{-}FlpIn}$ were transfected at 5 μg DNA each, using FuGene6. After 48 hr cells were treated with puromycin (1 μ g/mL) to remove un-transfected cells for a further 48 hr. Selected cells were replated at low density on 15 cm^2 plates to allow clonal growth in DMEM without puromycin. After 10 days clones were re-seeded and expanded. Clones were screened by PCR using primers that flank the SUMO4 gene using genomic DNA purified with direct PCR buffer (Viagen**)**. Clones that displayed reduced size of SUMO4 PCR product were sequenced by Sanger sequencing to confirm disruption of the SUMO4 locus. Western blot with FLAG was used to confirm the presence of stably integrated 3xFlagCas9. Clones that were positive for 3XFLAGCas9 were discarded to reduce the possibility of off-target editing by overexpressed Cas9 nuclease. SUMO4^{KO} clone 1.11 was used for generation of all complemented cell lines as for the parental U2OS$^{TrEx\text{-}FlpIn}$ cell line. Colony assays were performed as for (Garvin et al., 2019). For survival assays cells were seeded in 6 well plates and treated with doxycycline for 48 hr to induce expression of SUMO4. Cells were trypsinised and seeded onto 96 well plate at 1,000 cells / well for 24 hr prior to treatment. Cells were treated with indicated drug concentration for 72 hr before staining and fixing with crystal violet (0.5% in 50% methanol**)**, dried and resuspended in 10% acetic acid and absorption measured at 570 nm on a Multiscan SkyHigh plate reader (Thermo Fisher). Survival was measured as a % relative to untreated

wells. *SceI* reporter assays using His-HA-RFP SUMO4 were carried out as for (Garvin et al., 2019).

Transfection and plasmids

DNA transfections were performed using FuGene6 (Promega) at 4 μl FuGENE/ 1 μg DNA on 40% confluent cells. Transfection of siRNA were typically at 10 nM per sequence. Where two sequences were used per transcript 5 nM of each siRNA was used, for dual depletions a total of 10 nM of each siRNA was used to make 20 nM total. Dharmafect-1 was used at a concentration of 1 μL per mL of media. 6xHis-HA SUMO4 cDNA (NM_001002255.2) was generated by GenScript to include synonymous mutations that render it insensitive to siRNA #2 and siRNA #3. 6xHis-HA SUMO4 was subcloned into pcDNA5/FRT/TO using HindIII-BamHI sites. 6xHis-HA SUMO4 non siRNA resistant contains the original cDNA without siRNA resistance. 6xHis-HA-mRFP SUMO4 were subcloned from the pCDNA5/FRT/TO vector to pcDNA3.1 mRFP using HindIII - XhoI sites. FLAG-HA SUMO4 constructs were generated using primers that replaced the 6xHis tag with FLAG epitope and were cloned into pCDNA5/FRT/TO using HindIII - XhoI sites. Human SENP1 cDNA (ENST00000448372.5) was synthesised by GenScript to contain an N terminal FLAG tag and synonymous siRNA resistance mutations to the exon 6 and 12 siRNA used (see table 1). The cDNA also has synonymous mutations to remove BamHI, XhoI and NcoI sites and is cloned into pCDNA5/FRT/TO using BamHI - XhoI sites. Human Abraxas and BRCC36 cDNA have synonymous mutations to silence restriction sites and render siRNA resistance and were cloned into pCDNA5/FRT/TO using KpnI - XhoI.

Western blots, vinyl-sulfone labelling, turnover kinetics

Vinyl-sulfone labelling (VS), U2OS cells plated on 10 cm^2 dishes were treated as indicated for 48 hr before pelleting in ice old PBS and lysis in 1 mL of buffer (150 mM NaCl 10 mM HEPES pH 7.8, 10 mM KCl, 1.5 mM $MgCl_2$, 340mM Sucrose, 10% glycerol 0.2% NP40, protease and phosphatase inhibitor cocktails) followed by sonication and clarification by centrifugation. HA-SUMO-VS (Biotechne) were diluted in PBS and added at a final concentration of 10 ng in a volume of 100 μL for 20 min incubation at room temperature. Reactions were stopped by the addition of 6x Laemmli buffer and boiled. Turnover kinetics, for each condition 2x10 cm^2 dishes of U2OS ($1x10^6$ cell) were plated, siRNA transfected, and doxycycline treated for 48 hr. Cells were pelleted in PBS a control for each condition was lysed in 1 mL of buffer (250 mM NaCl 10 mM HEPES pH 7.8, 10 mM KCl, 1.5 mM $MgCl_2$, 340 mM Sucrose, 10% glycerol 0.2% NP40, protease and phosphatase inhibitor cocktails) containing 200 mM IAA. After vigorous mixing by pipette for 30 seconds 150 μL of sample was added to 50 μL of Laemmli buffer. For turnover cells were lysed in buffer without IAA, mixed by pipetting and 150 μL samples mixed at indicated times with Laemmli to stop deconjugation, samples were subsequently sonicated and boiled.

Immunofluorescence

U2OS were plated at 2.5 x 10^4 cells/well on 13 mm glass coverslips in 24 well plates (Corning) and attached overnight prior to siRNA depletion for 48 hours. For pre-extraction after 1x PBS

wash cells were treated with 250 µL / well ice cold CSK buffer (100 mM NaCl, 300 mM sucrose, 3 mM $MgCl_2$, 0.7% Triton-X100 and 10 mM PIPES) for 30 seconds prior to fixation with 4% Paraformaldehyde (PFA) in PBS at room temperature for 10 minutes. For non-pre-extracted samples cells were fixed in 4% PFA at room temperature for 10 minutes followed by permeabilisation with 0.5% Triton in PBS for 5 minutes. Coverslips were blocked with 5% FBS in PBS for 1 hour at room temperature followed by incubation with primary antibodies at 1 µg/mL (or 1:1000 for recombinant and CST MAbs) overnight at 4 °C in 5% FBS. Coverslips were washed twice with PBS followed by incubation with Alexa-Fluor 555 conjugated secondary antibodies at 1:2500 for 2 hours at room temperature in the dark. Cells were washed twice with PBS prior to incubation with 250 µL of Hoechst (1 µg/mL) for 2 minutes. Coverslips were mounted on slides using Immuno-Mount (Thermo Scientific) and sealed. Imaging was carried out on a Leica DM6000B microscope using an HBO lamp with 100W mercury short arc UV bulb light source. Images were captured at each wavelength sequentially using the Plan Apochromat HCX 100x/1.4 Oil objective at a resolution of 1392x1040 pixels.

Mass-spec

HEK293, 7x 10 cm^2 plates per condition treated with doxycycline, were transfected with 4 µg / plate 6XHis-HA SUMO4 WT, QFI-A and M55V for 72 hr prior to irradiation at 4 Gy or were left untreated. Cells were lysed 1 hr post irradiation. For lysis, cells were scraped in ice cold PBS, pelleted, and lysed in buffer (150 mM NaCl 10 mM HEPES pH 7.8, 10 mM KCl, 1.5 mM $MgCl_2$, 340mM Sucrose, 10% glycerol 0.2% NP40, protease and phosphatase inhibitor cocktails, 200 mM Iodoacetamide). Lysates were sonicated and clarified by centrifugation. Cleared lysates were incubated with HA magnetic agarose (Pierce) overnight with gentle agitation at 4C. Beads were washed 4x for 5 minutes each with lysis buffer followed by elution by boiling in 6X Laemmli buffer. Samples were separated on 4-20% Tris-Glycine bolt wedgewell gels (Invitrogen). Gels were stained using InstaBlue Coomassie and each sample divided into 10 slices. Gel slices were prepared using the Qiagen BioRobot 3000 prior to trypsin digestion and peptide extraction. UltiMate 3000 HPLC series (Dionex) was used for peptide concentration and separation. Samples were trapped on precolumn, Acclaim PepMap 100 C18, 5 µm, 100A 300 µm i.d. x 5mm (Dionex) and separated in Nano Series™ Standard Columns 75 µm i.d. x 15 cm^2, packed with C18 PepMap100, 3 µm, 100Å (Dionex). The gradient used was from 3.2% to 44% solvent B (0.1% formic acid in acetonitrile) for 30 min. The column was then washed with 90 % mobile phase B before re-equilibrating at 3.2 % mobile phase B. Peptides were eluted directly (~ 350 nL min-1) via a Triversa Nanomate nanospray source (Advion Biosciences) into a QExactive HF Orbitrap mass spectrometer (Thermo Fisher Scientifi**c)**. The spray voltage of QE HF was set to 1.7 kV through Triversa NanoMate and heated capillary at 275 °C. The mass spectrometer performed a full FT-MS scan (m/z 380−1600) and subsequent HCD MS/MS scans of the 20 most abundant ions with dynamic exclusion setting 15S. Full scan mass spectra were recorded at a resolution of 120,000 at m/z 200 and ACG target of 3×10^6. Precursor ions were fragmented in HCD MS/MS with resolution set up at 15,000 and a normalized collision energy of 28. ACG target for HCD MS/MS was 1x 10^5. The width of the precursor isolation window was 1.2 m/z and only multiply charged precursor ions were selected for MS/MS. Spectra were acquired for 56 min. The MS and MS/MS scans were searched against Uniprot database using Protein Discovery 2.2 software, Sequest HT algorithm (Thermo Fisher). Variable modifications were deamidation (N

and Q), oxidation (M) and phosphorylation (S, T and Y). The precursor mass tolerance was 10 ppm, and the MS/MS mass tolerance was 0.02Da. Two missed cleavage was allowed, and data were filtered with a false discovery rate (FDR) of 0.01. Proteins with at least two high confidence peptides are listed.

Supplementary tables

Table 1 – siRNA

siRNA name	Sequence
NTC (Renilla Luciferase)	CUUACGCUGAGUACUUCGA [dT][dT] [Phos]UCGAAGUACUCAGCGUAAG [dT][dT]
RAD51 Ex9	CCCUUUACAGAACAGACUA [dT][dT] [Phos]UAGUCUGUUCUGUAAAGGG [dT][dT]
RAD51 Ex11	UGAAGCUAUGUUCGCCAUU [dT][dT] [Phos]AAUGGCGAACAUAGCUUCA [dT][dT]
SUMO1 Ex2	CUCAAAGUCAUUGGACAGGAU [dT][dT] [Phos]AUCCUGUCCAAUGACUUUGAG [dT][dT]
SUMO1 UTR	CCUUCAUAUUACCCUCUCCUU [dT][dT] [Phos]AAGGAGAGGGUAAUAUGAAGG [dT][dT]
SUMO2 UTR A	GUACGUAGCUGUUACAUGU [dT][dT] [Phos]ACAUGUAACAGCUACGUAC [dT][dT]
SUMO2 UTR B	GCGUCUUGUUGUUUAAAUA [dT][dT] [Phos]UAUUUAAACAACAAGACGC [dT][dT]
SUMO3 Ex2	GCAAGCUGAUGAAGGCCUA [dT][dT] [Phos]UAGGCCUUCAUCAGCUUGC [dT][dT]
SUMO3 UTR	GGGAUGAAUCUGUAACUUA [dT][dT] [Phos]UAAGUUACAGAUUCAUCCC [dT][dT]
SUMO4 #2	ACCUCCCGUAGGCUGUUGAAA [dT][dT] [Phos]UUUCAACAGCCUACGGGAAGGU [dT][dT]
SUMO4 #3	ACUGUGCAGGUUUGUCUGUUC [dT][dT] [Phos]GAACAGACAAACCUGCACAGU [dT][dT]
SENP1 Ex6	CCGAAAGACCUCAAGUGGAUU [dT][dT] [Phos]AAUCCACUUGAGGUCUUUCGG [dT][dT]
SENP1 Ex12	CCGAAAGACCUCAAGUGGAUU [dT][dT] [Phos]AAUCCACUUGAGGUCUUUCGG [dT][dT]
SENP2 Ex4	ACAAUGCUGCCAGCUUAUUUG [dT][dT] [Phos]CAAAUAAGCUGGCAGCAUUGU [dT][dT]
SENP2 Ex13	GAGGAGAUAUUCAGACAUU [dT][dT] [Phos]AAUGUCUGAAUAUCUCCUC [dT][dT]
SENP3 Ex1	CCUCGCUGACAUUCCACUGGA[dT][dT] [Phos]UCCAGUGGAAUGUCAGCGAGG
SENP5 Ex2	CCUUACCAGAACAUCGUUCUA [dT][dT] [Phos]UAGAACGAUGUUCUGGUAAGG [dT][dT]
SENP5 UTR	CACUAUUGUUACCUCAAAUUU [dT][dT] [Phos]AAAUUUGAGGUAACAAUAGUG [dT][dT]
SENP6 Ex	CACAGGAUUAACAACCAAGAA [dT][dT] [Phos]UUCUUGGUUGUUAAUCCUGUG [dT][dT]
SENP7 Ex5	AUGUCCUAUGGACGGAUUUAG [dT][dT] [Phos]CUAAAUCCGUCCAUAGGACAU [dT][dT]
SENP7 Ex14	GAAUUGAAGCUGAAAGAUAUU [dT][dT]

	[Phos]AAUAUCUUUCAGCUUCAAUUC [dT][dT]
UBC9 Ex8	AGCAGAGGCCUACACGAUUUA [dT][dT] [Phos]UAAAUCGUGUAGGCCUCUGCU
UBC9 Ex9	AGAAGUUUGCGCCCUCAUAAG [dT][dT] [Phos]CUUAUGAGGGCGCAAACUUCU [dT][dT]
UBC13	SMARTPool L-003920-00-0005
RNF8	UGGACAAUUAUGGACAACA [dT][dT] [Phos]UGUUGUCCAUAAUUGUCCA [dT][dT]
RNF168 UTR	GCUGCUCUCUAGGCACACUCA [dT][dT] [Phos]UGAGUGUGCCUAGAGAGCAGC [dT][dT]
RAP80 Ex7	CCAUUGCUGAAAGCCUGAAUA [dT][dT] [Phos]UAUUCAGGCUUUCAGCAAUGG
RAP80 UTR	AUAGUGGUCCCUAGUUCAUUG [dT][dT] [Phos]CAAUGAACUAGGGACCACUAU [dT] [dT
RNF4 Ex9	UCACAUAUACGUCUCUGUC [dT][dT] [Phos]GACAGAGACGUAUAUGUGA [dT][dT]
RNF4 Ex11	AACGAUGAGACGUCCAUUC [dT][dT] [Phos]GAAUGGACGUCUCAUCGUU [dT][dT]

Table 2 – antibodies

Antibody	Catalogue number	Supplier	Concentration / Use
FLAG (Gt)	ab1257	Abcam	1:1000 (WB)
FLAG M2 (Ms)	F1804	Sigma	1:2000 (WB, IF)
GAPDH 6C5 (Ms)	CB1001	Calbiochem	1:5000 (WB)
HA.11 (Ms)	901501	Biolegend	1:1000 (WB, IF)
53BP1 (Gt)	AF1877	R&D System	1:2000 (IF)
53BP1 (Rb)	ab36823	Abcam	1:2000 (IF)
PML C7 (Ms)	ab96051	Abcam	1:1000 (IF)
PML (Rb)	PA5-79835	Invitrogen	1:1000 (IF)
SENP1 (Rb)	ab108981	Abcam	1:1000 (WB)
SENP3 (Rb)	ab124790	Abcam	1:1000 (WB)
SENP6 (Rb)	HPA024376	Merck	1:1000 (WB)
SUMO1 Y299 (Rb)	ab32058	Abcam	1:1000 (WB, IF)
SUMO1 21C7 (Ms)	33-2411	Invitrogen	1:500 (WB, IF)
SUMO2/3 8A2 (Ms)	ab81371	Abcam	1:1000 (WB, IF)
SUMO2/3 12F3 (Ms)	ASM23	Cytoskeleton	1:1000 (WB, IF)
H2AX-pSer139 (Ms)	ab2893	Abcam	1:2000 (IF)
H2AX-pSer139 (Rb)	ab22551	Abcam	1:2000 (IF)
MDC1 (Rb)	PLA-0016	Bethyl	1:1000 (IF)
MYC (Ms)	ab32	Abcam	1:1000 (IF)
Vinculin (Rb)	ab129002	Abcam	1:2000 (WB)
BARD1 (Rb)	ab64164	Abcam	1:1000 (IF)
RPA32-pSer33	ab211877	Abcam	1:1000 (IF)
RAD51 (Rb)	PC130	Calbiochem	1:1000 (IF)
SP100 (Rb)	HPA017384	Atlas	1:1000 (IF)
RAP80 (Rb)	NBP1-87156	Novus	1:1000 (IF)
BRCC36 (Rb)	3418-1	Epitomics	1:1000 (WB)
Ubc9	ab75854	Abcam	1:500 (WB)
Goat α Mouse AF 488	A11001	LifeTech	1:2000 (IF)
Goat α Rabbit AF 488	A11008	LifeTech	1:2000 (IF)
Goat α Mouse AF 555	A21422	LifeTech	1:2000 (IF)
Goat α Rabbit AF 555	A21428	LifeTech	1:2000 (IF)
Rabbit α Mouse HRP	P0161	DAKO	1:10,000 (WB)
Swine α Rabbit HRP	P0217	DAKO	1:10,000 (WB)

Table 3 - drugs

Chemical / Treatment	Manufacturer / Product code	Dosage / Time
Camptothecin (CPT)	Merck 208925	1 μM 2 hr
Doxycycline	Merck D9891	1 μg/ mL 72 hr
Cisplatin	Selleck S1166	1 μM 2 hr
Olaparib	Selleck S1060	10 μM 2 hr
Hygromycin B	Invitrogen H044-81VS	100 μg/ mL
Iodoacetamide (IAA)	Merck I1149	200 mM
Ionising Radiation	CellRad Irradiator (Precision X Ray)	4 Gy
ML-792	Selleck S8697	1 μM 3 hr

BEKES, M., PRUDDEN, J., SRIKUMAR, T., RAUGHT, B., BODDY, M. N. & SALVESEN, G. S. 2011. The dynamics and mechanism of SUMO chain deconjugation by SUMO-specific proteases. *J Biol Chem,* 286**,** 10238-47.

BOHREN, K. M., NADKARNI, V., SONG, J. H., GABBAY, K. H. & OWERBACH, D. 2004. A M55V polymorphism in a novel SUMO gene (SUMO-4) differentially activates heat shock transcription factors and is associated with susceptibility to type I diabetes mellitus. *J Biol Chem,* 279**,** 27233-8.

BRUNINGHOFF, K., AUST, A., TAUPITZ, K. F., WULFF, S., DORNER, W. & MOOTZ, H. D. 2020. Identification of SUMO Binding Proteins Enriched after Covalent Photo-Cross-Linking. *ACS Chem Biol,* 15**,** 2406-2414.

COLEMAN, K. A. & GREENBERG, R. A. 2011. The BRCA1-RAP80 Complex Regulates DNA Repair Mechanism Utilization by Restricting End Resection. *Journal of Biological Chemistry,* 286**,** 13669-13680.

COOPER, E. M., CUTCLIFFE, C., KRISTIANSEN, T. Z., PANDEY, A., PICKART, C. M. & COHEN, R. E. 2009. K63-specific deubiquitination by two JAMM/MPN plus complexes: BRISC-associated Brcc36 and proteasomal Poh1. *Embo Journal,* 28**,** 621-631.

DANIELSEN, J. R., POVLSEN, L. K., VILLUMSEN, B. H., STREICHER, W., NILSSON, J., WIKSTROM, M., BEKKER-JENSEN, S. & MAILAND, N. 2012. DNA damage-inducible SUMOylation of HERC2 promotes RNF8 binding via a novel SUMO-binding Zinc finger. *Journal of Cell Biology,* 197**,** 179-187.

DANTUMA, N. P. & VAN ATTIKUM, H. 2016. Spatiotemporal regulation of posttranslational modifications in the DNA damage response. *EMBO J,* 35**,** 6-23.

DHINGRA, N. & ZHAO, X. 2019. Intricate SUMO-based control of the homologous recombination machinery. *Genes Dev,* 33**,** 1346-1354.

DOU, H., HUANG, C., SINGH, M., CARPENTER, P. B. & YEH, E. T. 2010. Regulation of DNA repair through deSUMOylation and SUMOylation of replication protein A complex. *Mol Cell,* 39**,** 333-45.

FRADET-TURCOTTE, A., CANNY, M. D., ESCRIBANO-DIAZ, C., ORTHWEIN, A., LEUNG, C. C. Y., HUANG, H., LANDRY, M. C., KITEVSKI-LEBLANC, J., NOORDERMEER, S. M., SICHERI, F. & DUROCHER, D. 2013. 53BP1 is a reader of the DNA-damage-induced H2A Lys 15 ubiquitin mark. *Nature,* 499**,** 50-+.

GALANTY, Y., BELOTSERKOVSKAYA, R., COATES, J. & JACKSON, S. P. 2012. RNF4, a SUMO-targeted ubiquitin E3 ligase, promotes DNA double-strand break repair. *Genes & Development,* 26**,** 1179-1195.

GALANTY, Y., BELOTSERKOVSKAYA, R., COATES, J., POLO, S., MILLER, K. M. & JACKSON, S. P. 2009. Mammalian SUMO E3-ligases PIAS1 and PIAS4 promote responses to DNA double-strand breaks. *Nature,* 462**,** 935-9.

GARVIN, A. J. 2019. Beyond reversal: ubiquitin and ubiquitin-like proteases and the orchestration of the DNA double strand break repair response. *Biochem Soc Trans,* 47**,** 1881-1893.

GARVIN, A. J., DENSHAM, R., BLAIR-REID, S. A., PRATT, K. M., STONE, H. R., WEEKES, D., LAWRENCE, K. J. & MORRIS, J. R. 2013. The deSUMOylase SENP7 promotes chromatin relaxation for homologous recombination DNA repair. *Embo Reports,* 14**,** 975-983.

GARVIN, A. J., LANZ, A. & MORRIS, J. R. 2022. SUMO monoclonal antibodies vary in sensitivity, specificity, and ability to detect SUMO conjugate types. *bioRxiv***,** 2022.03.19.484974.

GARVIN, A. J. & MORRIS, J. R. 2017. SUMO, a small, but powerful, regulator of double-strand break repair. *Philosophical Transactions of the Royal Society B-Biological Sciences,* 372.

GARVIN, A. J., WALKER, A. K., DENSHAM, R. M., CHAUHAN, A. S., STONE, H. R., MACKAY, H. L., JAMSHAD, M., STAROWICZ, K., DAZA-MARTIN, M., RONSON, G. E., LANZ, A. J., BEESLEY, J. F. & MORRIS, J. R. 2019. The deSUMOylase SENP2 coordinates homologous recombination and nonhomologous end joining by independent mechanisms. *Genes & Development,* 33**,** 333-347.

GONZALEZ-PRIETO, R., EIFLER-OLIVI, K., CLAESSENS, L. A., WILLEMSTEIN, E., XIAO, Z., TALAVERA ORMENO, C. M. P., OVAA, H., ULRICH, H. D. & VERTEGAAL, A. C. O. 2021. Global non-covalent SUMO interaction networks reveal SUMO-dependent stabilization of the non-homologous end joining complex. *Cell Rep,* 34**,** 108691.

GUO, D., HAN, J., ADAM, B. L., COLBURN, N. H., WANG, M. H., DONG, Z., EIZIRIK, D. L., SHE, J. X. & WANG, C. Y. 2005. Proteomic analysis of SUMO4 substrates in HEK293 cells under serum starvation-induced stress. *Biochem Biophys Res Commun,* 337**,** 1308-18.

GUO, D. H., LI, M. Y., ZHANG, Y., YANG, P., ECKENRODE, S., HOPKINS, D., ZHENG, W. P., PUROHIT, S., PODOLSKY, R. H., MUIR, A., WANG, J. Z., DONG, Z., BRUSKO, T., ATKINSON, M., POZZILLI, P., ZEIDLER, A., RAFFEL, L. J., JACOB, C. O., PARK, Y., SERRANO-RIOS, M., LARRAD, M. T. M., ZHANG, Z. X., GARCHON, H. J., BACH, J. F., ROTTER, J. I., SHE, J. X. & WANG, C. Y. 2004. A functional variant of SUMO4, a new I kappa B alpha modifier, is associated with type 1 diabetes. *Nature Genetics,* 36**,** 837-841.

GUZZO, C. M., BERNDSEN, C. E., ZHU, J. M., GUPTA, V., DATTA, A., GREENBERG, R. A., WOLBERGER, C. & MATUNIS, M. J. 2012. DNA DAMAGE RNF4-Dependent Hybrid SUMO-Ubiquitin Chains Are Signals for RAP80 and Thereby Mediate the Recruitment of BRCA1 to Sites of DNA Damage. *Science Signaling,* 5.

GUZZO, C. M., RINGEL, A., COX, E., UZOMA, I., ZHU, H., BLACKSHAW, S., WOLBERGER, C. & MATUNIS, M. J. 2014. Characterization of the SUMO-Binding Activity of the Myeloproliferative and Mental Retardation (MYM)-Type Zinc Fingers in ZNF261 and ZNF198. *Plos One,* 9.

HARIHARASUDHAN, G., JEONG, S. Y., KIM, M. J., JUNG, S. M., SEO, G., MOON, J. R., LEE, S., CHANG, I. Y., KEE, Y., YOU, H. J. & LEE, J. H. 2022. TOPORS-mediated RAD51 SUMOylation facilitates homologous recombination repair. *Nucleic Acids Res,* 50**,** 1501-1516.

HE, X. Y., RICEBERG, J., SOUCY, T., KOENIG, E., MINISSALE, J., GALLERY, M., BERNARD, H., YANG, X. F., LIAO, H., RABINO, C., SHAH, P., XEGA, K., YAN, Z. H., SINTCHAK, M., BRADLEY, J., XU, H., DUFFEY, M., ENGLAND, D., MIZUTANI, H., HU, Z. G., GUO, J. P., CHAU, R., DICK, L. R., BROWNELL, J. E., NEWCOMB, J., LANGSTON, S., LIGHTCAP, E. S., BENCE, N. & PULUKURI, S. M. 2017. Probing the roles of SUMOylation in cancer cell biology by using a selective SAE inhibitor. *Nature Chemical Biology,* 13**,** 1164-+.

HENDRIKS, I. A. & VERTEGAAL, A. C. O. 2016. A comprehensive compilation of SUMO proteomics. *Nature Reviews Molecular Cell Biology,* 17**,** 581-595.

HU, X., PAUL, A. & WANG, B. 2012. Rap80 Protein Recruitment to DNA Double-strand Breaks Requires Binding to Both Small Ubiquitin-like Modifier (SUMO) and Ubiquitin Conjugates. *Journal of Biological Chemistry,* 287**,** 25510-25519.

KAKAROUGKAS, A., ISMAIL, A., KATSUKI, Y., FREIRE, R., SHIBATA, A. & JEGGO, P. A. 2013. Co-operation of BRCA1 and POH1 relieves the barriers posed by 53BP1 and RAP80 to resection. *Nucleic acids research,* 41**,** 10298-311.

KOLLI, N., MIKOLAJCZYK, J., DRAG, M., MUKHOPADHYAY, D., MOFFATT, N., DASSO, M., SALVESEN, G. & WILKINSON, K. D. 2010. Distribution and paralogue specificity of mammalian deSUMOylating enzymes. *Biochemical Journal,* 430**,** 335-344.

KUMAR, R., GONZALEZ-PRIETO, R., XIAO, Z., VERLAAN-DE VRIES, M. & VERTEGAAL, A. C. O. 2017. The STUbL RNF4 regulates protein group SUMOylation by targeting the SUMO conjugation machinery. *Nat Commun,* 8**,** 1809.

LASCORZ, J., CODINA-FABRA, J., REVERTER, D. & TORRES-ROSELL, J. 2021. SUMO-SIM interactions: From structure to biological functions. *Semin Cell Dev Biol*.

LEE, D., APELT, K., LEE, S. O., CHAN, H. R., LUIJSTERBURG, M. S., LEUNG, J. W. C. & MILLER, K. M. 2022. ZMYM2 restricts 53BP1 at DNA double-strand breaks to favor BRCA1 loading and homologous recombination. *Nucleic Acids Res*.

LI, Y. H., LUO, K. T., YIN, Y. J., WU, C. M., DENG, M., LI, L., CHEN, Y. P., NOWSHEEN, S., LOU, Z. K. & YUAN, J. 2017a. USP13 regulates the RAP80-BRCA1 complex dependent DNA damage response. *Nature Communications,* 8.

LI, Y. Y., WANG, H., YANG, X. X., GENG, H. Y., GONG, G., KIM, H. J., ZHOU, Y. H. & WU, J. J. 2017b. Small Ubiquitin-Like Modifier 4 (SUMO4) Gene M55V Polymorphism and Type 2 Diabetes Mellitus: A Meta-analysis Including 6,823 Subjects. *Front Endocrinol (Lausanne),* 8**,** 303.

LIN, H. Y., WANG, C. L., HSIAO, P. J., LU, Y. C., CHEN, S. Y., LIN, K. D., HSIN, S. C., HSIEH, M. C. & SHIN, S. J. 2007. SUMO4 M55V variant is associated with diabetic nephropathy in type 2 diabetes. *Diabetes,* 56**,** 1177-80.

LOMBARDI, P. M., MATUNIS, M. J. & WOLBERGER, C. 2017. RAP80, ubiquitin and SUMO in the DNA damage response. *J Mol Med (Berl),* 95**,** 799-807.

LUO, K. T., ZHANG, H. X., WANG, L. W., YUAN, J. & LOU, Z. K. 2012. Sumoylation of MDC1 is important for proper DNA damage response. *Embo Journal,* 31**,** 3008-3019.

MERRILL, J. C., MELHUISH, T. A., KAGEY, M. H., YANG, S. H., SHARROCKS, A. D. & WOTTON, D. 2010. A role for non-covalent SUMO interaction motifs in Pc2/CBX4 E3 activity. *PLoS ONE,* 5**,** e8794.

MORRIS, J. R., BOUTELL, C., KEPPLER, M., DENSHAM, R., WEEKES, D., ALAMSHAH, A., BUTLER, L., GALANTY, Y., PANGON, L., KIUCHI, T., NG, T. & SOLOMON, E. 2009. The SUMO modification pathway is involved in the BRCA1 response to genotoxic stress. *Nature,* 462**,** 886-90.

NG, H. M., WEI, L. Z., LAN, L. & HUEN, M. S. Y. 2016. The Lys(63)-deubiquitylating Enzyme BRCC36 Limits DNA Break Processing and Repair. *Journal of Biological Chemistry,* 291**,** 16197-16207.

NOSO, S., IKEGAMI, H., FUJISAWA, T., KAWABATA, Y., ASANO, K., HIROMINE, Y., TSURUMARU, M., SUGIHARA, S., LEE, I., KAWASAKI, E., AWATA, T. & OGIHARA, T. 2005. Genetic heterogeneity in association of the SUMO4 M55V variant with susceptibility to type 1 diabetes. *Diabetes,* 54**,** 3582-6.

OWERBACH, D., MCKAY, E. M., YEH, E. T. H., GABBAY, K. H. & BOHREN, K. M. 2005. A proline-90 residue unique to SUMO-4 prevents maturation and sumoylation. *Biochemical and Biophysical Research Communications,* 337**,** 517-520.

PATTERSON-FORTIN, J., SHAO, G., BRETSCHER, H., MESSICK, T. E. & GREENBERG, R. A. 2010. Differential Regulation of JAMM Domain Deubiquitinating Enzyme Activity within the RAP80 Complex. *Journal of Biological Chemistry,* 285**,** 30971-30981.

PFEIFFER, A., LUIJSTERBURG, M. S., ACS, K., WIEGANT, W. W., HELFRICHT, A., HERZOG, L. K., MINOIA, M., BOTTCHER, C., SALOMONS, F. A., VAN ATTIKUM, H. & DANTUMA, N. P. 2017. Ataxin-3 consolidates the MDC1-dependent DNA double-strand break response by counteracting the SUMO-targeted ubiquitin ligase RNF4. *EMBO J*.

PICHLER, A., FATOUROS, C., LEE, H. & EISENHARDT, N. 2017. SUMO conjugation - a mechanistic view. *Biomol Concepts,* 8**,** 13-36.

PSAKHYE, I. & JENTSCH, S. 2012. Protein group modification and synergy in the SUMO pathway as exemplified in DNA repair. *Cell,* 151**,** 807-20.

SCHICK, M., ZHANG, L., MAURER, S., MAURER, H. C., ISAAKAIDIS, K., SCHNEIDER, L., PATRA, U., SCHUNCK, K., ROHLEDER, E., HOFSTETTER, J., BALUAPURI, A., SCHERGER, A. K., SLOTTA-

HUSPENINA, J., HETTLER, F., WEBER, J., ENGLEITNER, T., MARESCH, R., SLAWSKA, J., LEWIS, R., ISTVANFFY, R., HABRINGER, S., STEIGER, K., BAIKER, A., OOSTENDORP, R. A. J., MIETHING, C., LENHOF, H. P., BASSERMANN, F., CHAPUY, B., WIRTH, M., WOLF, E., RAD, R., MULLER, S. & KELLER, U. 2022. Genetic alterations of the SUMO isopeptidase SENP6 drive lymphomagenesis and genetic instability in diffuse large B-cell lymphoma. *Nat Commun,* 13**,** 281.

SEDIMBI, S. K., LUO, X. R., SANJEEVI, C. B., SWEDISH CHILDHOOD DIABETES STUDY, G., DIABETES INCIDENCE IN SWEDEN STUDY, G., LERNMARK, A., LANDIN-OLSSON, M., ARNQVIST, H., BJORCK, E., NYSTROM, L., OHLSON, L. O., SCHERSTEN, B., OSTMAN, J., AILI, M., BAATH, L. E., CARLSSON, E., EDENWALL, H., FORSANDER, G., GRANSTROM, B. W., GUSTAVSSON, I., HANAS, R., HELLENBERG, L., HELLGREN, H., HOLMBERG, E., HORNELL, H., IVARSSON, S. A., JOHANSSON, C., JONSELL, G., KOCKUM, K., LINDBLAD, B., LINDH, A., LUDVIGSSON, J., MYRDAL, U., NEIDERUD, J., SEGNESTAM, K., SJOBLAD, S., SKOGSBERG, L., STROMBERG, L., STAHLE, U., THALME, B., TULLUS, K., TUVEMO, T., WALLENSTEEN, M., WESTPHAL, O., DAHLQUIST, G. & AMAN, J. 2007. SUMO4 M55V polymorphism affects susceptibility to type I diabetes in HLA DR3- and DR4-positive Swedish patients. *Genes Immun,* 8**,** 518-21.

SHAO, G., LILLI, D. R., PATTERSON-FORTIN, J., COLEMAN, K. A., MORRISSEY, D. E. & GREENBERG, R. A. 2009. The Rap80-BRCC36 de-ubiquitinating enzyme complex antagonizes RNF8-Ubc13-dependent ubiquitination events at DNA double strand breaks. *Proceedings of the National Academy of Sciences of the United States of America,* 106**,** 3166-71.

SHIRE, K., WONG, A. I., TATHAM, M. H., ANDERSON, O. F., RIPSMAN, D., GULSTENE, S., MOFFAT, J., HAY, R. T. & FRAPPIER, L. 2016. Identification of RNF168 as a PML nuclear body regulator. *J Cell Sci,* 129**,** 580-91.

SOBHIAN, B., SHAO, G. Z., LILLI, D. R., CULHANE, A. C., MOREAU, L. A., XIA, B., LIVINGSTON, D. M. & GREENBERG, R. A. 2007. RAP80 targets BRCA1 to specific ubiquitin structures at DNA damage sites. *Science,* 316**,** 1198-1202.

TONG, Z., QI, J., MA, W., WANG, D., HU, B., LI, Y., JIA, X., PENG, J., WANG, Z. & ZHONG, M. 2021. SUMO4 Gene SNP rs237025 and the Synergistic Effect With Weight Management: A Study of Risk Factors and Interventions for MetS. *Front Genet,* 12**,** 786393.

TSURUMARU, M., KAWASAKI, E., IDA, H., MIGITA, K., MORIUCHI, A., FUKUSHIMA, K., FUKUSHIMA, T., ABIRU, N., YAMASAKI, H., NOSO, S., IKEGAMI, H., AWATA, T., SASAKI, H. & EGUCHI, K. 2006. Evidence for the role of small ubiquitin-like modifier 4 as a general autoimmunity locus in the Japanese population. *J Clin Endocrinol Metab,* 91**,** 3138-43.

TYPAS, D., LUIJSTERBURG, M. S., WIEGANT, W. W., DIAKATOU, M., HELFRICHT, A., THIJSSEN, P. E., VAN DEN BROEK, B., MULLENDERS, L. H. & VAN ATTIKUM, H. 2016. The de-ubiquitylating enzymes USP26 and USP37 regulate homologous recombination by counteracting RAP80 (vol 43, pg 6919, 2015). *Nucleic Acids Research,* 44**,** 2976-2976.

VAREJAO, N., LASCORZ, J., LI, Y. & REVERTER, D. 2020. Molecular mechanisms in SUMO conjugation. *Biochem Soc Trans,* 48**,** 123-135.

VYAS, R., KUMAR, R., CLERMONT, F., HELFRICHT, A., KALEV, P., SOTIROPOULOU, P., HENDRIKS, I. A., RADAELLI, E., HOCHEPIED, T., BLANPAIN, C., SABLINA, A., VAN ATTIKUM, H., OLSEN, J. V.,

JOCHEMSEN, A. G., VERTEGAAL, A. C. O. & MARINE, J. C. 2013. RNF4 is required for DNA double-strand break repair in vivo. *Cell Death and Differentiation,* 20**,** 490-502.

WEI, W. Z., YANG, P., PANG, J. F., ZHANG, S., WANG, Y., WANG, M. H., DONG, Z., SHE, J. X. & WANG, C. Y. 2008. A stress-dependent SUMO4 sumoylation of its substrate proteins. *Biochemical and Biophysical Research Communications,* 375**,** 454-459.

WU, Q., PAUL, A., SU, D., MEHMOOD, S., FOO, T. K., OCHI, T., BUNTING, E. L., XIA, B., ROBINSON, C. V., WANG, B. & BLUNDELL, T. L. 2016. Structure of BRCA1-BRCT/Abraxas Complex Reveals Phosphorylation-Dependent BRCT Dimerization at DNA Damage Sites. *Mol Cell,* 61**,** 434-448.

WU, X., LIU, S., SAGUM, C., CHEN, J., SINGH, R., CHATURVEDI, A., HORTON, J. R., KASHYAP, T. R., FUSHMAN, D., CHENG, X., BEDFORD, M. T. & WANG, B. 2019. Crosstalk between Lys63- and Lys11-polyubiquitin signaling at DNA damage sites is driven by Cezanne. *Genes Dev,* 33**,** 1702-1717.

YIN, Y. L., SEIFERT, A., CHUA, J. S., MAURE, J. F., GOLEBIOWSKI, F. & HAY, R. T. 2012. SUMO-targeted ubiquitin E3 ligase RNF4 is required for the response of human cells to DNA damage. *Genes & Development,* 26**,** 1196-1208.

ZHANG, Q., LIU, D., ZHAO, Z. Y., SUN, Q., DING, L. X. & WANG, Y. X. 2017. Association between the SUMO4 M55V Polymorphism and Susceptibility to Type 2 Diabetes Mellitus: A Meta-analysis. *Biomed Environ Sci,* 30**,** 288-295.

Figure 1

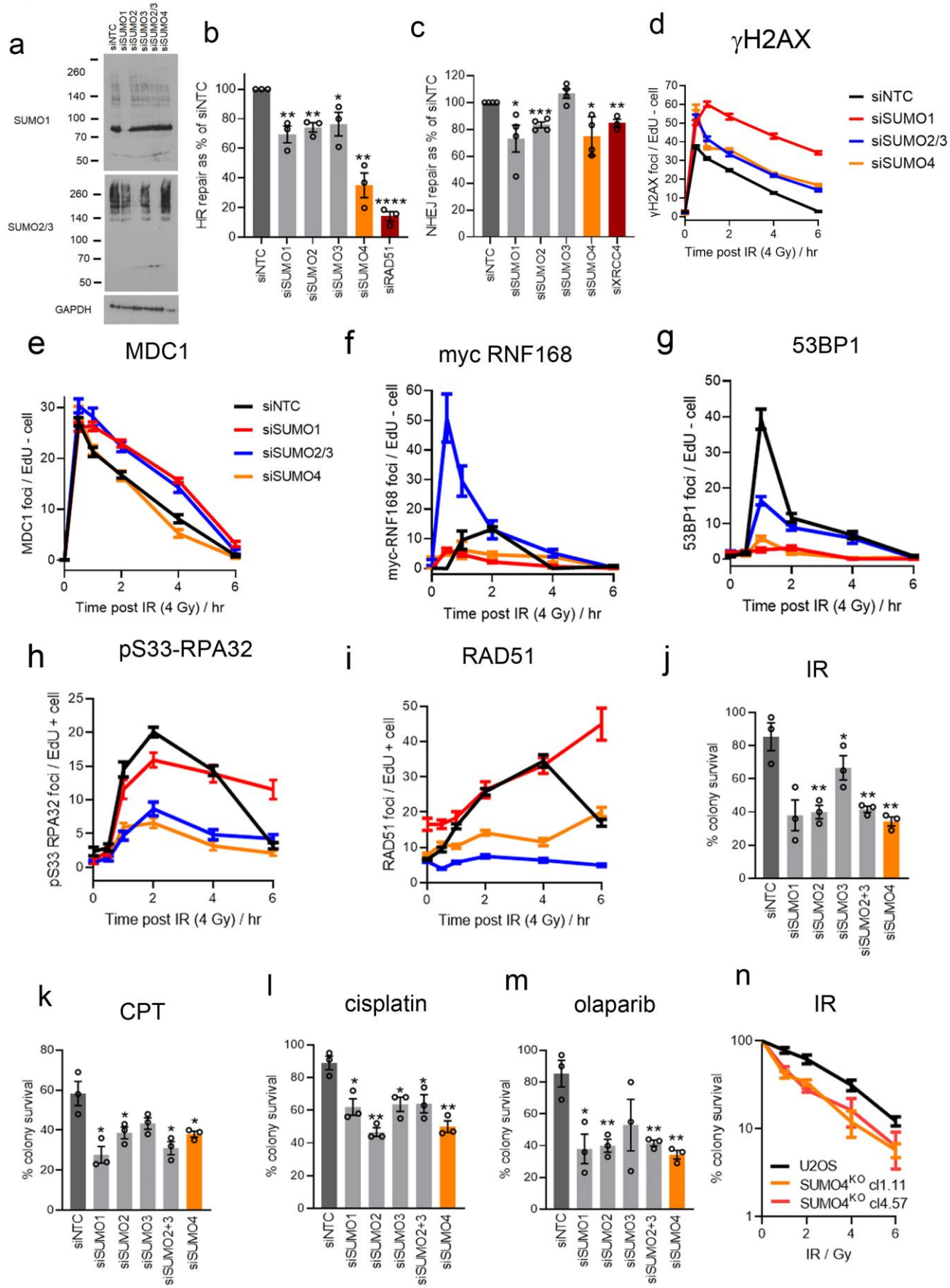

Figure 1

a) Western blot of cells treated with siRNA to SUMO1 (siSUMO1) and to SUMO2 (siSUMO2) and SUMO3 (siSUMO3). The SUMO2/3 antibody detects both SUMO2 and SUMO3, with SUMO2 being the dominant isoform. siNTC is siRNA to non-targeting control (siNTC).

b-c) U2OS DR3 (HR reporter) or EJ5 (NHEJ reporter) co-transfected with siRNA and DNA for *SceI* and RFP as a transfection marker. Events were gated on RFP (*SceI* transfection) and GFP (repair reporter). Repair efficiency is calculated relative to siNTC/RFP transfected cells expressed as 100%. Error bars = SEM.

d) U2OS siRNA depleted with indicated siRNA for 48 hr prior to IR (4 Gy) and fixation at indicated times. Cells were incubated with EdU (10 μM) 30 min prior to irradiation. The number of γH2AX foci were counted in EdU negative and positive cells (Supplemental Figure 1a). N=~150 cells from 3 experimental repeats, bars denote SEM.

e) As for **d)** staining MDC1 foci

f) As for **d)** but using U2OS myc-RNF168 cells and immunostaining with myc antibody.

g) As for **d)** staining 53BP1 foci

h) as for **d)** staining phospho-Ser33 RPA32 foci in EdU positive cells

i) as for **d)** staining with RAD51 in EdU positive cells

j-m) colony survival in U2OS treated with indicated siRNA for 48 hours prior to treatment j) – 2 Gy IR, k) – 1 μM camptothecin (CPT), l) - 1 μM Cisplatin, m – 10 μM Olaparib. All drug treatments for 2 hr. Error bars show SEM, n=3. Statistical significance by two-tailed t-test between siNTC and siSUMO.

n) colony survival in parental U2OS^{FlpIn} and SUMO4^{KO} cl.1.11 (gRNA #1) and cl.4.57 (gRNA #4). Treated with IR at the indicated dose. N=3 error bars = SEM.

Figure 2

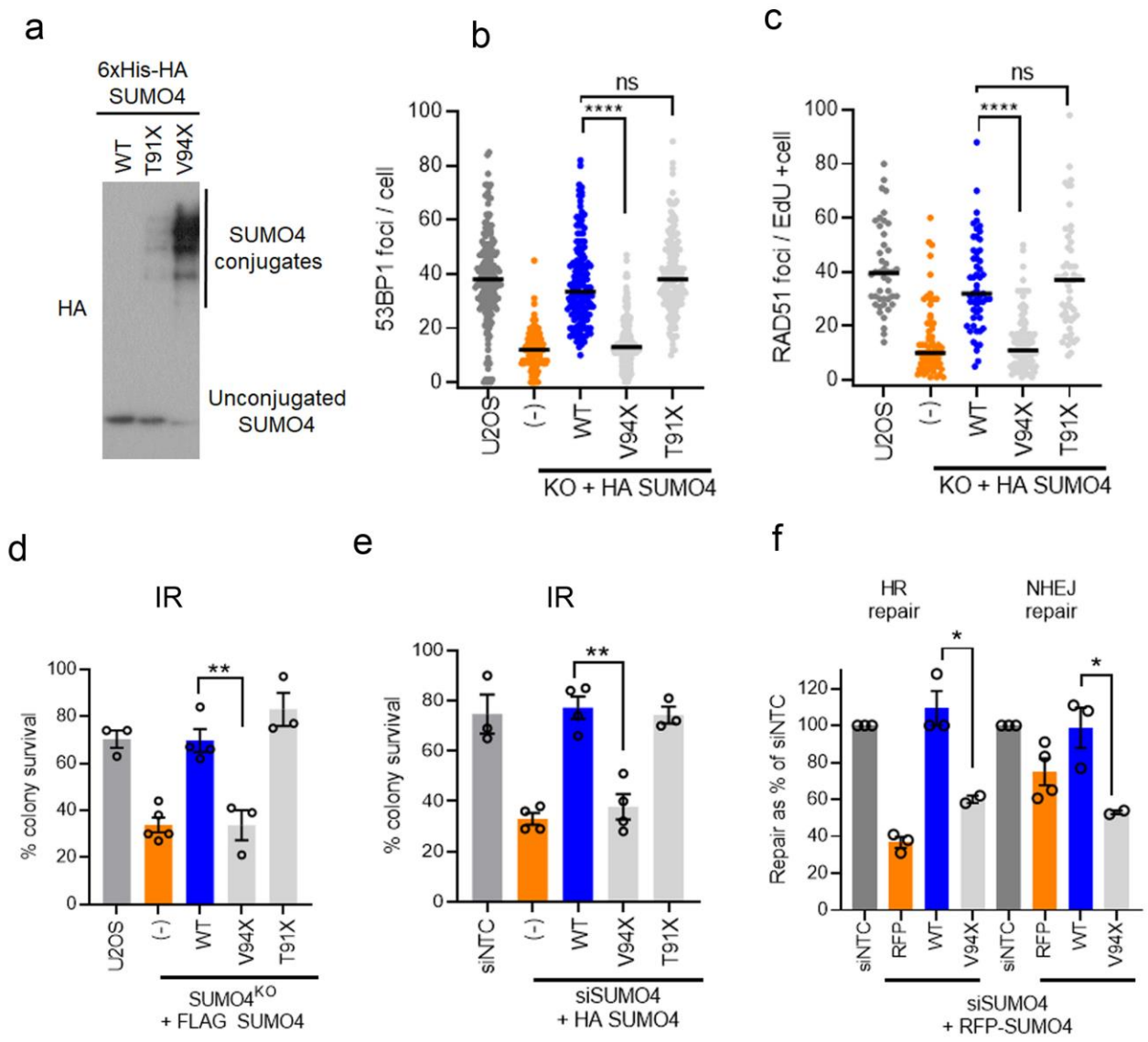

Figure 2

a) U2OS treated with doxycycline for 48 hrs to induce expression of 6xHis-HA SUMO4 WT, V94X (artificially matured and conjugatable) or T91X (truncated before di-Gly and un-conjugatable). Lysates were immunoblotted with HA antibody.

b) SUMO4^{KO} cells dox treated for 48 hr to induce HA-FLAG SUMO4 expression prior to IR treatment (4 Gy) and fixation 2 hr later followed by immunostaining for 53BP1 foci. N=~150 cells from 3 experiments, bars denote mean.

c) As for **b)** but for RAD51.

d) cells treated as for **b)** but treated with 2 Gy IR prior to plating for colony survival.

e) as for **d)** but with U2OS treated with siRNA against SUMO4 for 48 hr with concurrent dox treatment to induce expression of siRNA resistant 6xHis-HA SUMO4 cDNA.

f) U2OS DR3 (HR reporter) or EJ5 (NHEJ reporter) co-transfected with siRNA and DNA for *SceI* and RFP or RFP-SUMO4. Events gated on GFP (repair reporter) and RFP (positive transfection). Repair efficiency is calculated relative to siNTC/RFP transfected cells expressed as 100%. Error bars = SEM.

Figure 3

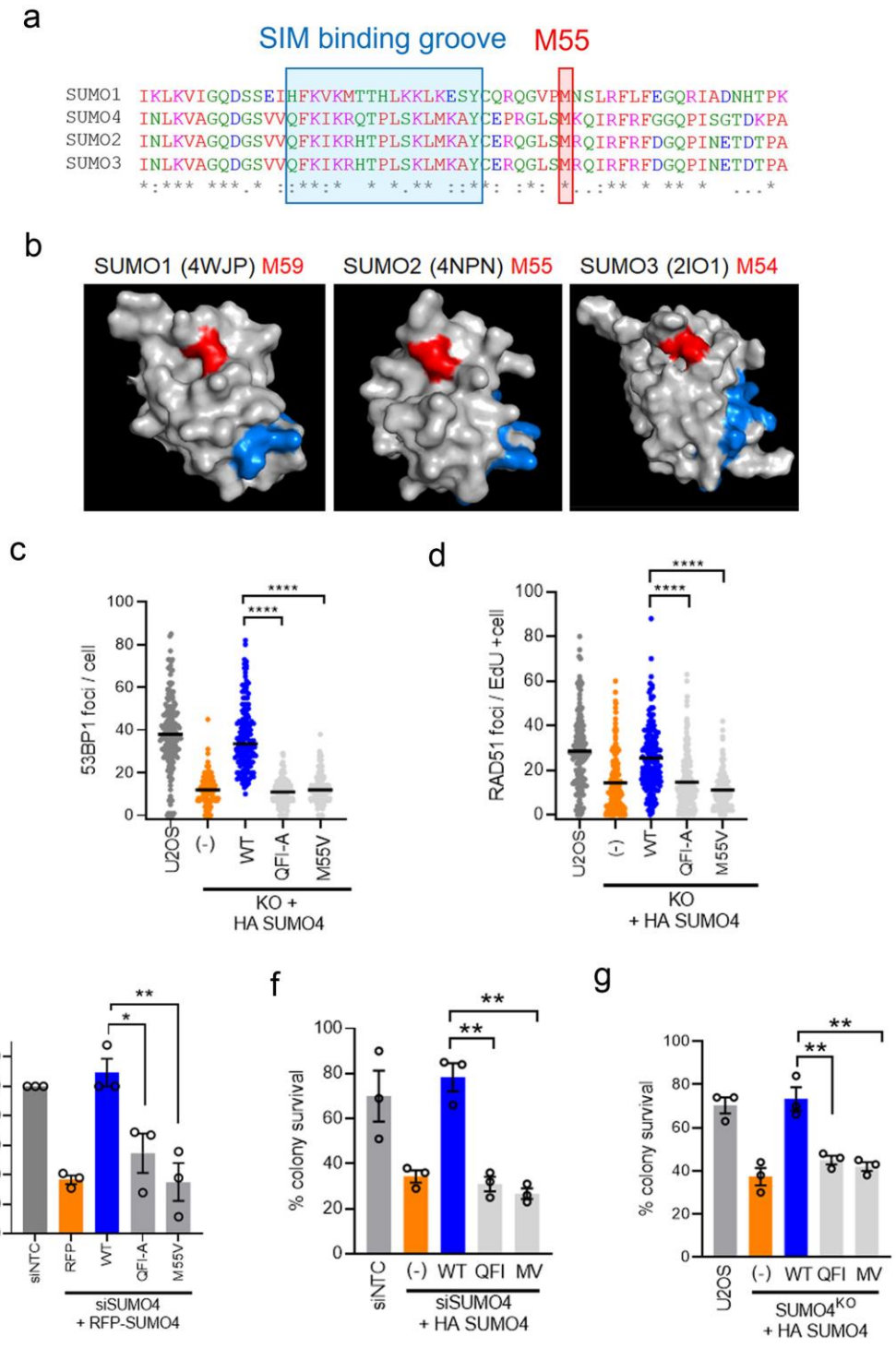

Figure 3

a) Alignment using Clustal Omega of human SUMO1 (aa 22-78), SUMO2 (aa 18-74), SUMO3 (aa 18-73) and SUMO4 (aa 18-74). The SIM binding groove is highlighted in blue and methionine 55 of SUMO4 in red.

b) Location of M55 highlighted in red (M54 in SUMO3 and M59 in SUMO1) on crystal structures of indicated SUMO isoforms. The SIM interacting groove is highlighted in blue.

c) U2OS SUMO4^{KO} cells complemented with HA-FLAG SUMO4 WT, QFI-A and M55V were treated with dox for 48 hours prior to IR (4 Gy) and fixed 2 hr later. 53BP1 foci number are scored / cell. The parental U2OS^{FlpIn} are used as controls. N= a total of ~ 200 cells from 3 experimental repeats. Bars denote mean.

d) As for **c)** but cells were pulsed with EdU 30 min prior to irradiation. RAD51 foci are scored in EdU positive cells only.

e) U2OS-DR3 cells were siRNA depleted of SUMO4 and transfected with *SceI*, RFP or RFP-SUMO4 simultaneously. Cells were gated on GFP/RFP positivity and are calculated relative to siNTC. N=3 experiments performed in triplicate.

f) Colony survival in U2OS siRNA depleted of SUMO4 and treated with doxycycline for 72 hours to express siRNA resistant SUMO4 cDNA. Cells were irradiated with 2 Gy, n=3.

g) as for **f)** but using doxycycline treated U2OS SUMO4^{KO} complemented with HA-FLAG SUMO4 cDNA, n=3.

Figure 4

a

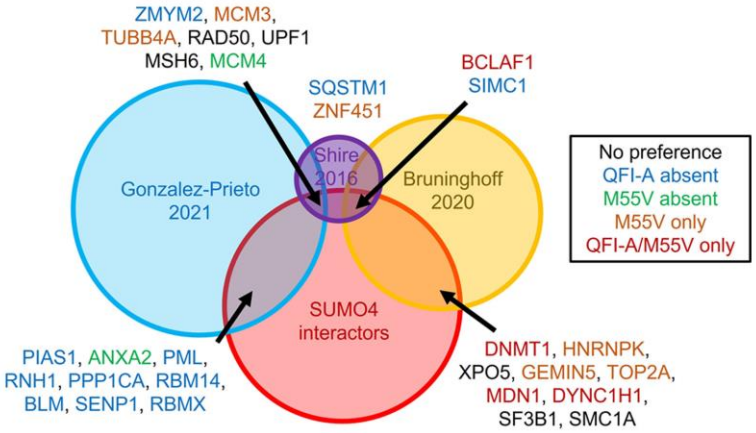

b

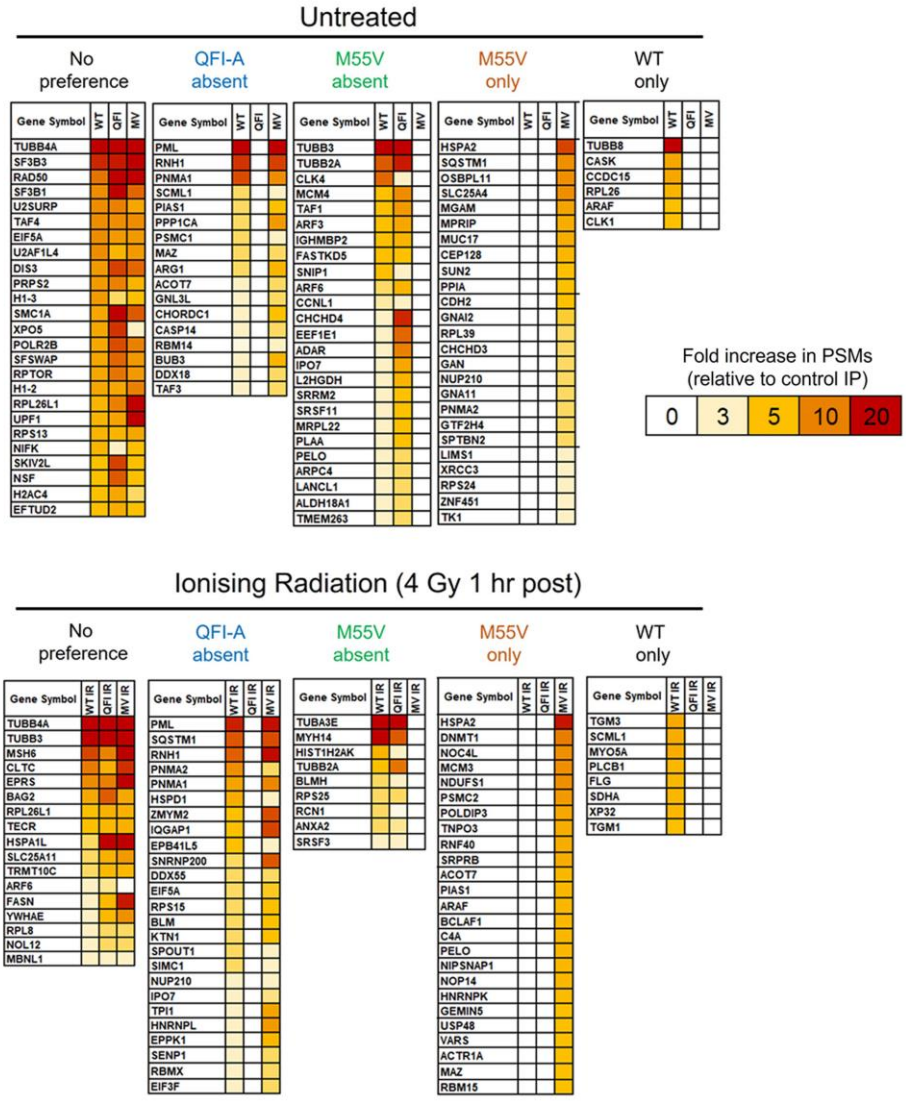

Figure 4

a) Venn diagram of SUMO4 interactors with published SUMO interaction datasets. All SUMO4 interactors in HEK293 (untreated and IR, WT, QFI-A and M55V) with a >3-fold enrichment of PSM is included in the SUMO4 dataset (n=500). The dataset from Shire 2016 (Shire et al., 2016) contains interactors of synthetic tetraSUMO2 constructs from HEK293 nuclear extracts (n=67). The Gonzalez-Prieto 2021 dataset (Gonzalez-Prieto et al., 2021) includes interactors of SUMO2 and triSUMO2 in HeLa (n= 587). The Bruninghoff 2020 (Bruninghoff et al., 2020) dataset includes cross linked interactors of SUMO2, diSUMO2 and triSUMO2 from HeLa nuclear lysates (n=337). Representative proteins at the intersections of each dataset are shown and are colour coded depending on their SUMO4 interaction.

b) Heat map of putative SUMO4 interactors in untreated and irradiated HEK293. Fold enrichment of PSMs between SUMO4 IP and respective control IP is shown from pale yellow (3x) to dark red (>20x). The interactors are divided by interaction with SUMO4 mutant, the top 25 most enriched proteins are shown for each group.

Figure 5

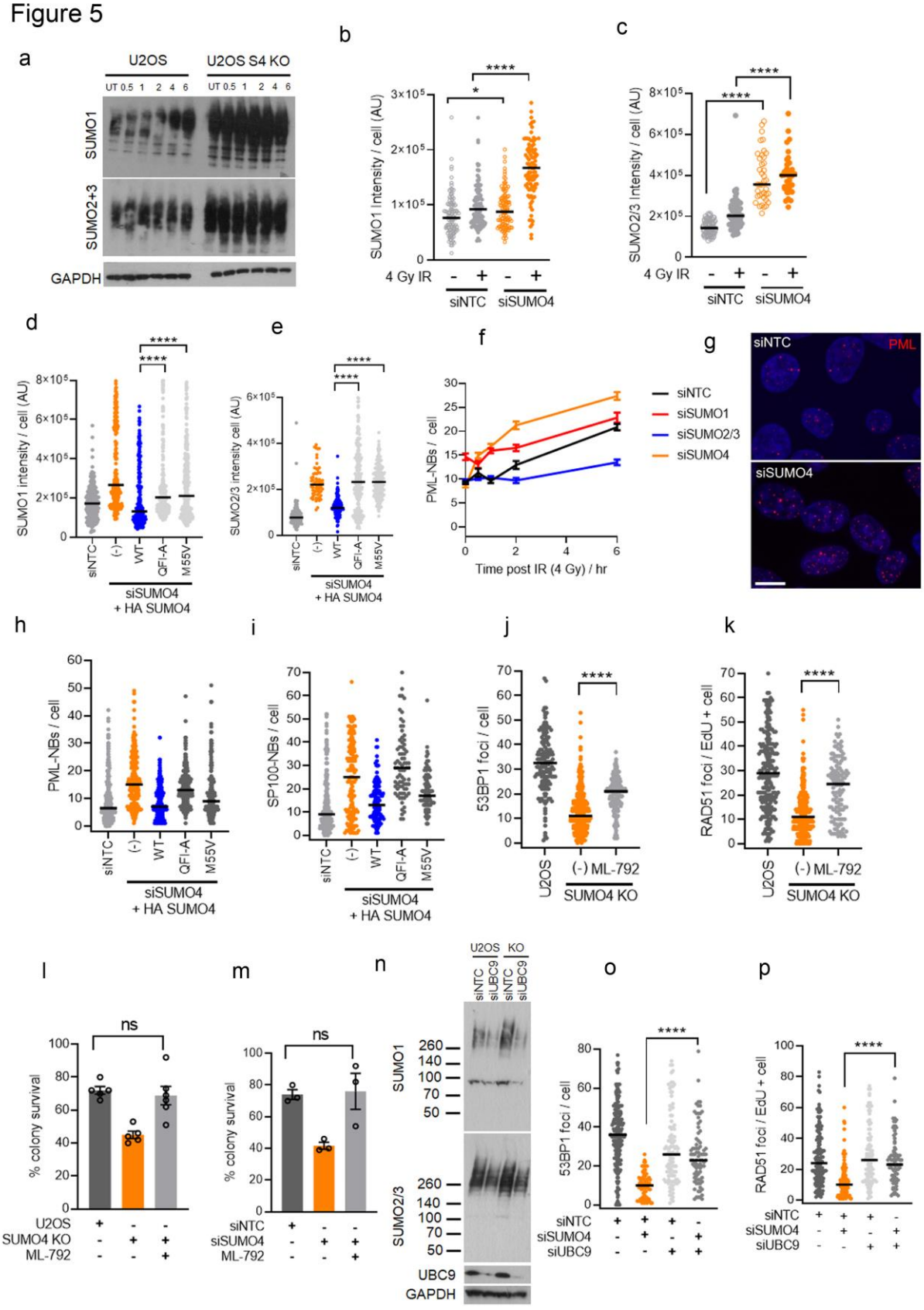

Figure 5

a) SUMO conjugates in whole cell lysates from U2OS or U2OS SUMO4^{KO} cells treated with 4 Gy IR and lysed at indicated time points.

b) U2OS or U2OS SUMO4^{KO} cells treated with 4 Gy IR and pre-extracted to remove soluble material and fixed at 2 hr, immunostained with SUMO1 antibody. Fluorescent intensity per cell is shown in arbitrary units (AU) from ~100 cells per condition.

c) as for **b)** but SUMO2/3 intensity.

d) U2OS treated with SUMO4 siRNA for 48 hr and doxycycline to induce HA-SUMO4 expression, followed by IR (4 Gy) treatment and fixation at 2 hr. N= ~150 cells. Cells were immunostained with SUMO1 antibody and quantified as for b)

e) As for **d)** but with SUMO2/3 intensity.

f) U2OS cells treated with indicated siRNA for 48 hr, treated with IR and fixed at indicated time points followed by immunostaining with PML antibody, n =~150 cells.

g) representative image of PML-NBs 2 hr post irradiation from non-targeting control and SUMO4 siRNA treated cells. Scale bar = 10 μm.

h) cells treated as for **d)** but with PML antibody immunostaining.

i) as for **d)** but with SP100 antibody.

j) U2OS SUMO4^{KO} cells treated with 1 μM ML-792 or DMSO for 1 hour prior to irradiation (4 Gy) and fixation 2 hr later, n = ~150 cells from 3 experiments.

k) as for **j)** but with a 30 min pulse of EdU before irradiation and immunostaining with RAD51 antibody.

l) Cells treated as for **j)** but plated immediately after IR (2 Gy) for colony survival, n =4.

m) as for **l)** but with a 48 hr treatment with SUMO4 siRNA.

n) Immunoblot of lysates from U2OS siRNA depleted for SUMO4 or UBC9 for 48 hr prior to irradiation (4 Gy) and fixation at 2 hr, n =~150.

o) Cells treated as for n) but with IR treatment (4 Gy) and fixation at 2 hr, followed by immunofluorescent detection of 53BP1 foci.

p) as for o) but with RAD51 foci in EdU labelled cells.

Figure 6

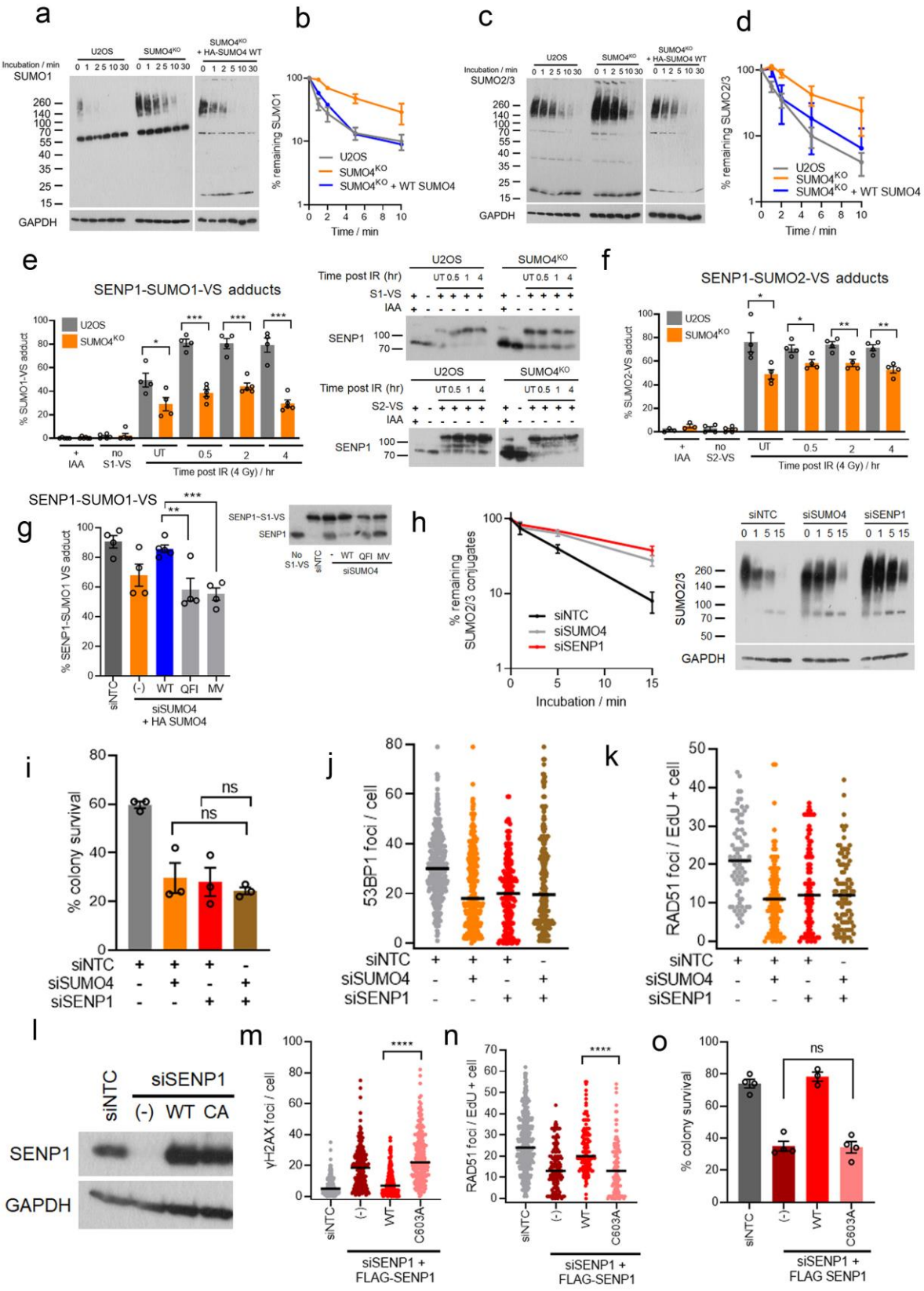

Figure 6

a) Immunoblot of SUMO1-conjugate loss in U2OS, SUMO4^{KO} or SUMO4^{KO} - HA-FLAG SUMO4 WT (doxycycline induced for 48 hr). Cells were lysed in buffer containing cysteine protease inhibitor IAA (200 mM) (0 time point) or buffer without IAA. A fraction of extract was removed at indicated times and denatured to stop further deconjugation. Lysates were blotted with SUMO1 antibody

b) quantification of **a)** from three experimental repeats. The % remaining SUMO1 is calculated by densitometry relative to the 0 control (lysed in buffer containing IAA and denatured immediately). Error bars = SEM.

c) SUMO2/3-conjugate loss as for **a)** but lysates probed with SUMO2/3 antibody

d) quantification of **c)**.

e) HA-SUMO1 vinyl sulfone labelling of SENP1 in cell extracts from U2OS or U2OS SUMO4^{KO} that had been either untreated (UT) or irradiated with (4 Gy). Reactions were immunoblotted with SENP1 antibody and the relative amount of upper band (SUMO1-VS labelled SENP1) versus unlabelled SENP1 (lower band) was calculated from 4 experiments. As controls, lysates were incubated with the cysteine protease inhibitor IAA to prevent labelling (+ IAA) or were not incubated with HA-SUMO1 vinyl-sulfone (no S1-VS). Representative panels of SENP1 blots are shown.

f) as for **e) but** using HA-SUMO2 vinyl sulfone labelling of SENP1 in SUMO4 deficient and complemented cells.

g) as for **e)** but with the addition of SUMO4^{KO} + WT, QFI-A or M55V SUMO4 cell lines induced with dox for 48 hr. Lysates were made and quantified as for **e)**. N=4. A representative immunoblot of SENP1 labelling is shown.

h) U2OS siRNA depleted for SENP1 or SUMO4 for 48 hr. Lysates were prepared as for **a)**. Error bars denote SEM, n=3. Representative panels of SUMO2/3 conjugates are shown.

i) Colony assays in U2OS treated with siRNA to SENP1, SUMO4 or both for 48 hr prior to irradiation (4 Gy). Error bars = SEM, n=3.

j) Cells treated as for **i)** but fixed 2 hr post IR (4 Gy) for immunostaining for 53BP1. N=~150 from 3 experiments. Bars denote mean.

k) as for **j)** but with RAD51 in EdU positive cells.

l) Immunoblot of SENP1 expression levels in U2OS siRNA treated to reduce endogenous SENP1 and complemented with either WT or C603A (CA) catalytic mutant siRNA resistant cDNA.

m) U2OS FLAG SENP1 cells siRNA depleted with SENP1, and doxycycline treated to induce WT or catalytic mutants (C603A) SENP1. Cells were fixed 2 hr post 4 Gy and immunostained with γH2AX antibody, n =~150 cells, bar denotes mean.

n) as for **l)** but for RAD51

o) colony survival in cells treated as for **l)** but with 2 Gy IR, n=4, error bars denote SEM

Figure 7

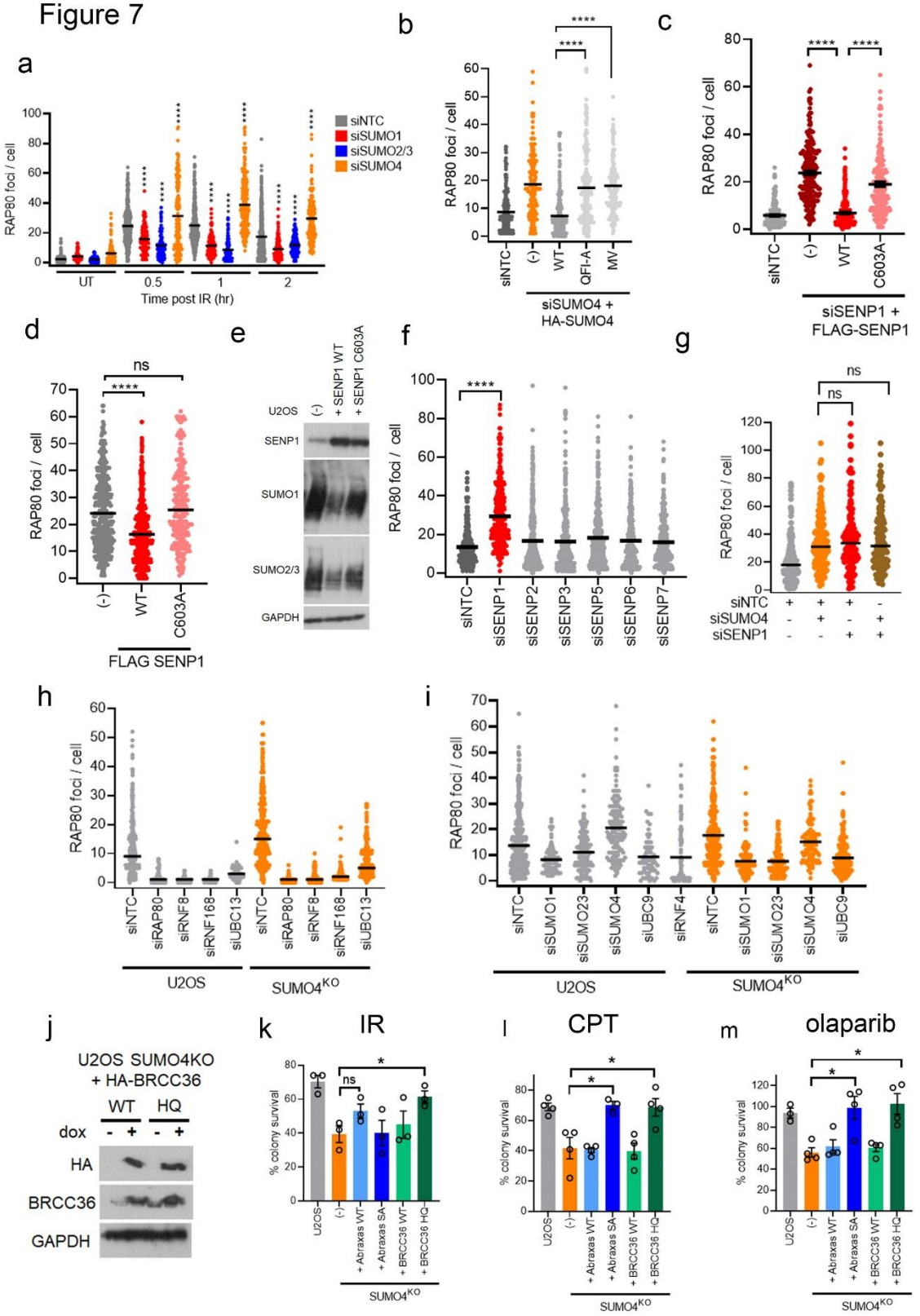

Figure 7

a) U2OS treated with indicated siRNA for 48 hr prior to irradiation (4 Gy) and fixation at indicated times followed by immunostaining with RAP80 antibody. Statistical difference by two tailed t-test between siNTC and siSUMO for each time point, n =~150 cells. Horizontal bars denote mean.

b) U2OS treated with SUMO4 siRNA and dox to induce expression of 6xHis-HA SUMO4 and mutants for 48 hr prior to irradiation (4 Gy) and fixation at 2 hr followed by immunostaining with RAP80 antibody. Statistical difference by two tailed t-test between SUMO4 WT and SUMO4 QFI-A or M55V complemented cells. N=~150 cells. Horizontal bars denote mean.

c) U2OS or U2OS FLAG SENP1 cells treated with SENP1 siRNA and dox to induce siRNA resistant FLAG-SENP1 expression for 48 hr followed by irradiation (4 Gy) and fixation 2 hr later. Statistical differences (two tailed t-test) between SENP1 depleted cells and SENP1 WT or C603A (catalytic mutant) complemented cells is shown. N~150 cells.

d) U2OS, U2OS FLAG SENP1 WT, or C603A cells were dox treated for 48 hr to induce SENP1 overexpression followed by IR (4 Gy) and fixation 2 hr later. N~200 cells, statistical difference by two tailed t-test. Horizontal bars denote mean.

e) Immunoblot of SENP1 over-expression from U2OS cells expressing dox induced FLAG-SENP1 WT or C603A catalytic mutant. The effects on total SUMO1 and SUMO2/3 conjugate levels are shown.

f) U2OS siRNA depleted with indicated SENP (SUMO protease) for 48 hr prior to IR (4 Gy) and fixation 2 hr later and immunostaining for RAP80 foci. N= ~150 cells from 3 experiments. Horizontal bars denote mean. Significance determined by two tailed t-test.

g) As for **f)** but with SENP1 and SUMO4 siRNA treatment.

h-**i)** U2OS and U2OS SUMO4^{KO} treated with indicated siRNA 48 hr prior to irradiation (4 Gy) and fixation 2 hr later. N~150 cells. Horizontal bars denote mean.

j) Immunoblot of HA and total BRCC36 levels in SUMO 4^{KO} cells overexpressing dox inducible HA-BRCC36 WT and HQ (catalytic deficient).

k-l-**m)** U2OS SUMO4^{KO} treated for 24 hr with dox to induce over-expression of FLAG-Abraxas WT, SA (S404A/S406A – BRCA1 interaction mutant) or HA-BRCC36 WT, HQ (H124Q/H126Q – catalytic mutant). Parental U2OS and SUMO4^{KO} were used as controls. Cells were treated with **i**- 2 Gy IR, **j**- 1 μM CPT / 2 hr, or **k**- 10 μM olaparib / 2 hr. N=3 (IR) or 4 (CPT and olaparib). Statistical difference by two tailed t-test is shown. Error bars = SEM.

Supplemental Figure 1

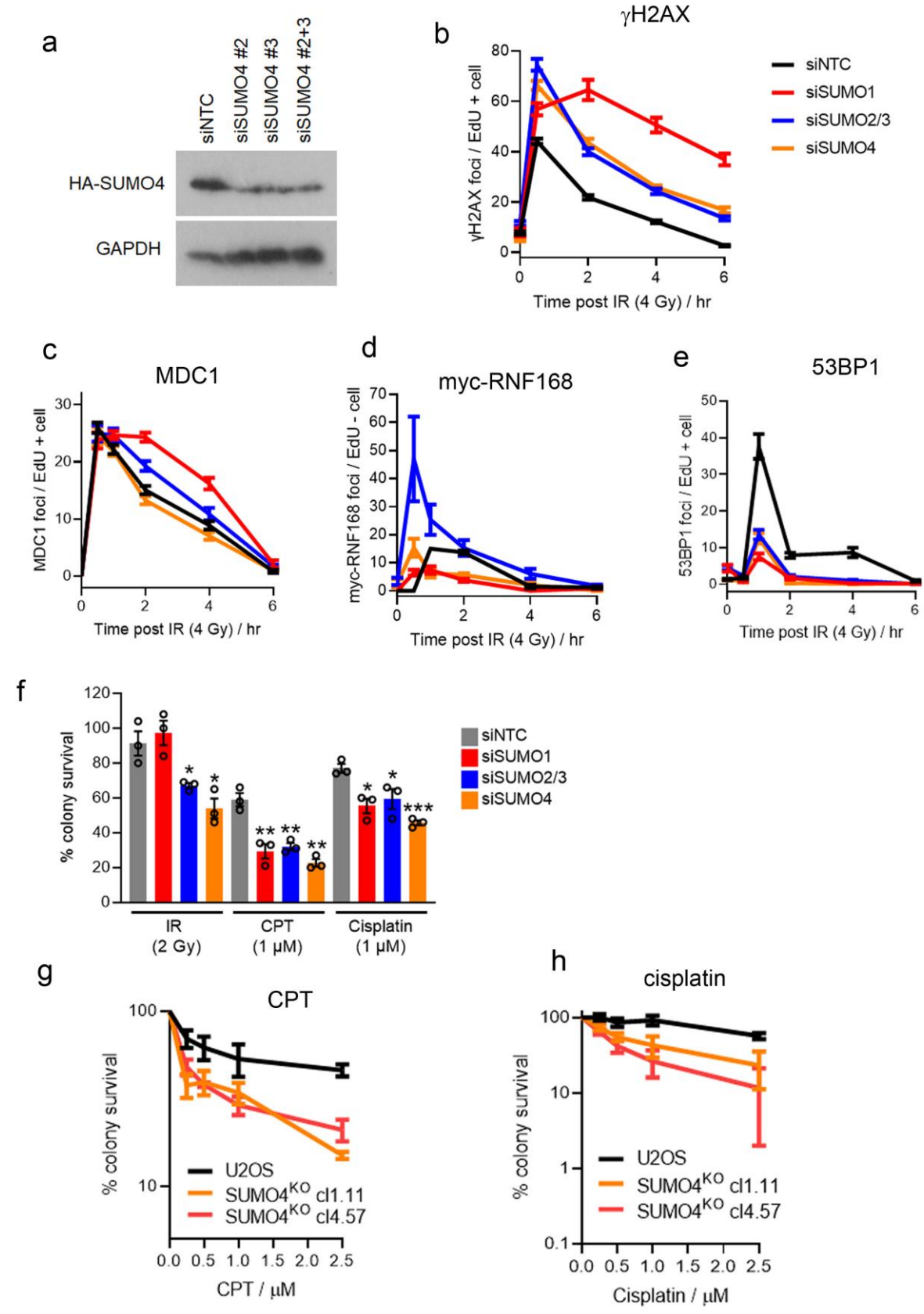

Supplemental Figure 1

a) Immunoblot of lysates from U2OS cells expressing 6xHis-HA SUMO4 WT (non siRNA resistant) cDNA following siRNA treatment and doxycycline treatment for 48 hr.

b) U2OS siRNA depleted with indicated siRNA for 48 hr prior to IR (4 Gy) and fixation at indicated times. Cells were incubated with EdU (10 m) 30 min prior to irradiation. The number of γH2AX foci were counted in EdU positive cells. N=~150 cells from 3 experimental repeats, bars denote SEM.

c) as for b) but with MDC1 foci in EdU positive (S phase) cells.

d) as for b) but with myc-RNF168 in EdU positive (S phase) cells.

e) as for b) but with 53BP1 in EdU positive (S phase) cells.

f) Colony survival in HeLa siRNA depleted with indicated siRNA for 48 hr prior to treatment with IR (2 Gy), CPT or cisplatin (1 μM 2hr). Error bars = SEM, n=3. Statistical significance is relative to the siNTC for each treatment using two tailed t-test.

g-**h)** colony survival in parental U2OS^{FlpIn} and SUMO4^{KO} cl.1.11 (gRNA #1) and cl.4.57 (gRNA #4). Treated with CPT (**g)** or cisplatin (**h)** at the indicated dose for 2 hr. N=3 error bars = SEM.

Supplemental Figure 2

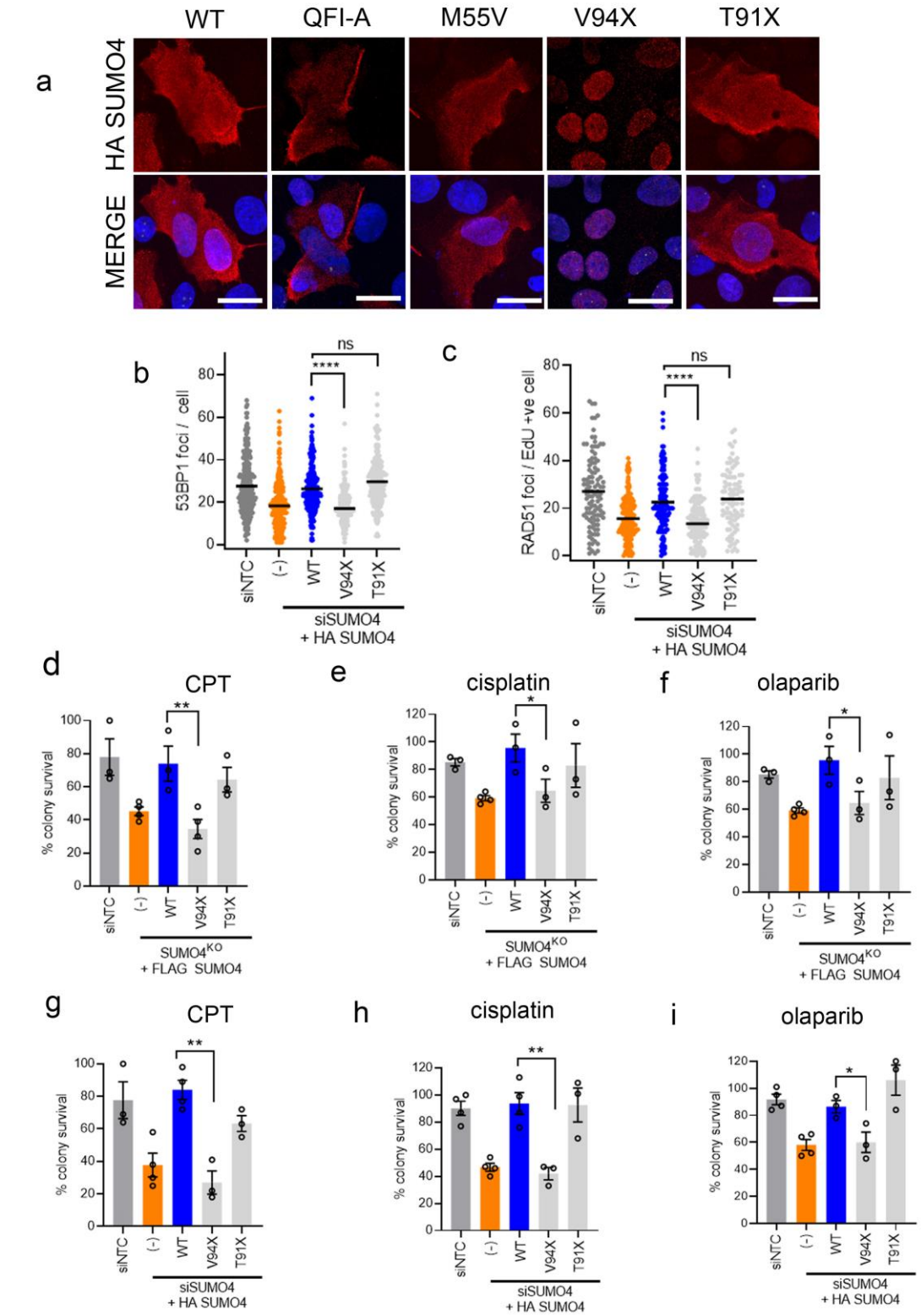

Supplemental Figure 2

a) Localisation of 6xHis-HA SUMO4 in U2OS treated with doxycycline to induce expression for 48 hours prior to fixation and immunostaining with HA antibody.

b-c) U2OS or U2OS – 6xHis-HA SUMO4 siRNA treated to deplete endogenous SUMO4 with concomitant dox addition to induce expression of siRNA resistant SUMO4 cDNA for 48 hr prior to IR (4 Gy) and fixation 2 hr later followed by immunostaining for 53BP1 (b) or RAD51 (c).

d-f) SUMO4^{KO} cells dox treated for 48 hr to induce HA-FLAG SUMO4 expression prior to treatment with **d)** CPT (1 μM), **e)** cisplatin (1 μM) or **f)** olaparib (10 μM) for 2 hr.

g-h) as for d-f) but using SUMO4 siRNA and dox to induce expression of siRNA resistant SUMO4 cDNA **g)** CPT (1 μM), **h)** cisplatin (1 μM) or **i)** olaparib (10 μM) for 2 hr.

Supplemental Figure 3

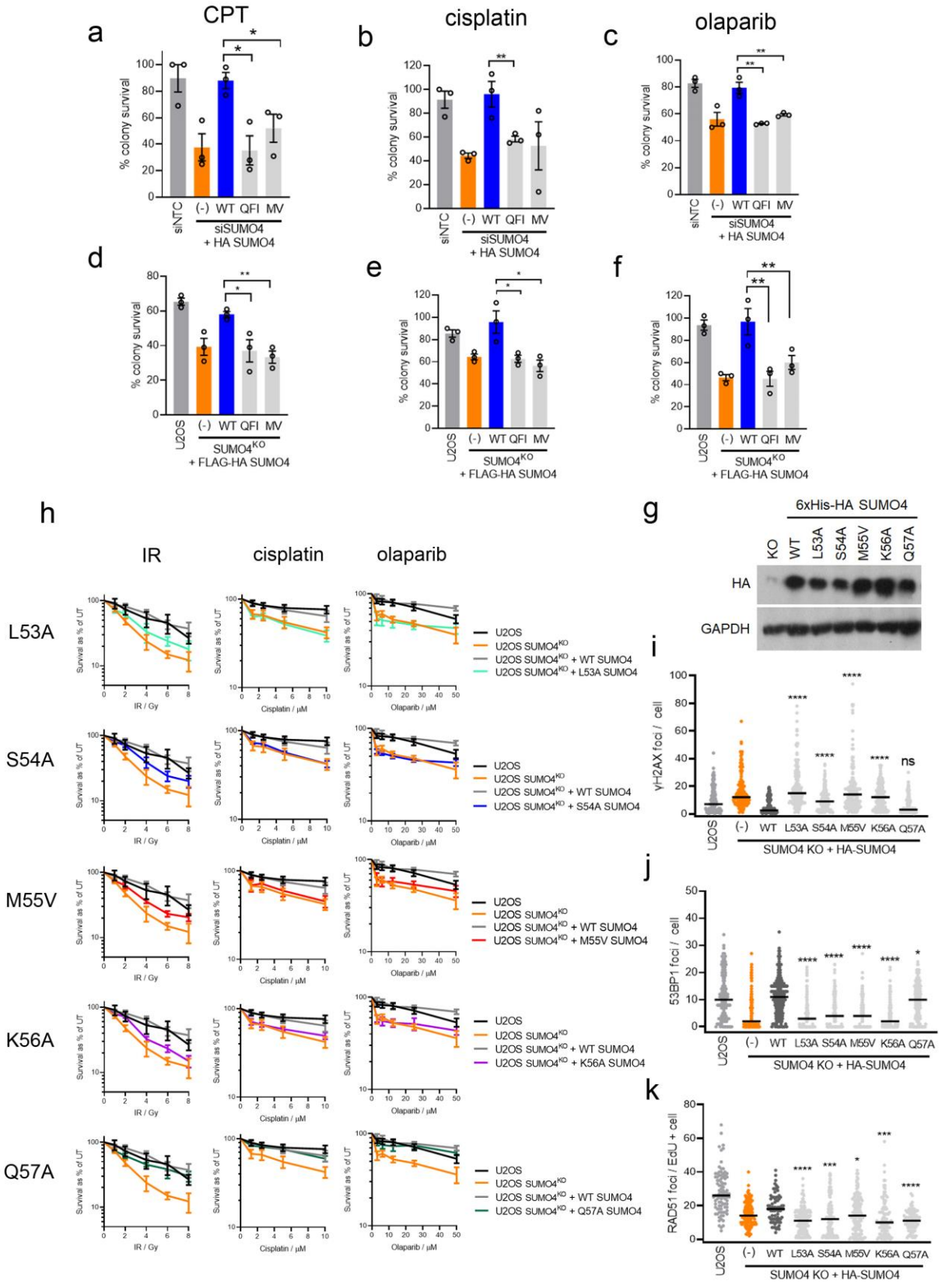

Supplemental Figure 3

a) Colony survival assay in 6xHis-HA SUMO4 complemented U2OS treated as for figure 3g but with CPT at 1 μM for 2 hours prior to plating.

b) as for **a)** but with 1 μM cisplatin.

c) as for **a)** but with 10 μM olaparib.

d-f) Colony survival in U2OS SUMO4^{KO} treated with doxycycline for 48 hours to express SUMO4 cDNA. Cells were treated the following 2 hr prior to plating d) CPT (1 μM), e) cisplatin (1 μM), or f) olaparib (10 μM).

g) Immunoblot of expression levels of 6xHis-HA SUMO4 in dox treated SUMO4^{KO} cells.

h) Survival assays using U2OS SUMO4^{KO} cells complemented by doxycycline treatment for 48 hr to induce expression of 6xHis-HA SUMO4. After doxycycline cells were either irradiated or treated with cisplatin or olaparib continuously for an additional 5 days. Cells were fixed and stained with crystal violet and measured by absorption. Survival is shown as a % relative to untreated controls. N=4.

i) Number of γH2AX foci / cell in U2OS SUMO4^{KO} cells treated with doxycycline to induce expression of 6xHis-HA SUMO4 for 48 hr prior to irradiation (4 Gy) and fixation 2 hr later. N= ~150 cells from 3 experimental repeats. Bars denote mean. Statistical significance by two tailed t-test is shown relative to the SUMO4 WT complemented cells.

j) as for **h)** but measuring 53BP1 foci.

k) as for **h)** but measuring RAD51 foci in EdU positive cells.

Supplemental Figure 4

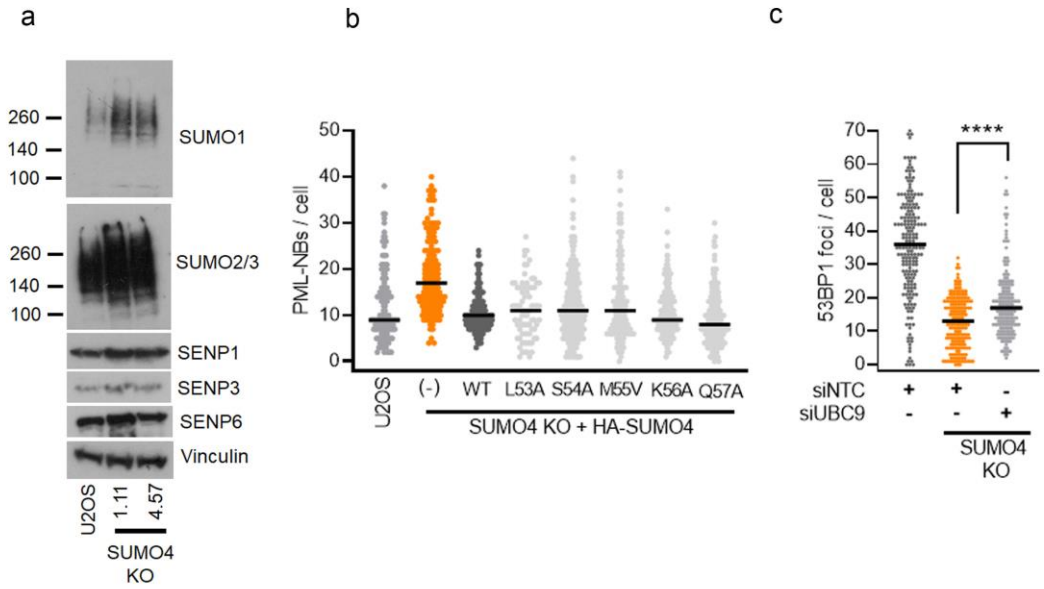

Supplemental Figure 4

a) SUMO1, SUMO2/3, SENP1,3 and 6 levels in whole cell lysates from two independent SUMO4^{KO} clones.

b) PML-NB numbers in U2OS SUMO4^{KO} cells doxycycline treated to induce 6xHis-HA SUMO4 for 48 hr prior to irradiation (4 Gy) and fixation 2 hr later. N=~150 cells from 3 experiments.

c) U2OS SUMO4^{KO} cells UBC9 siRNA depleted for 48 hr prior to IR (4 Gy) and fixation 2 hr later, followed by immunostaining for 53BP1 foci, n =~150 cells.

Supplemental Figure 5

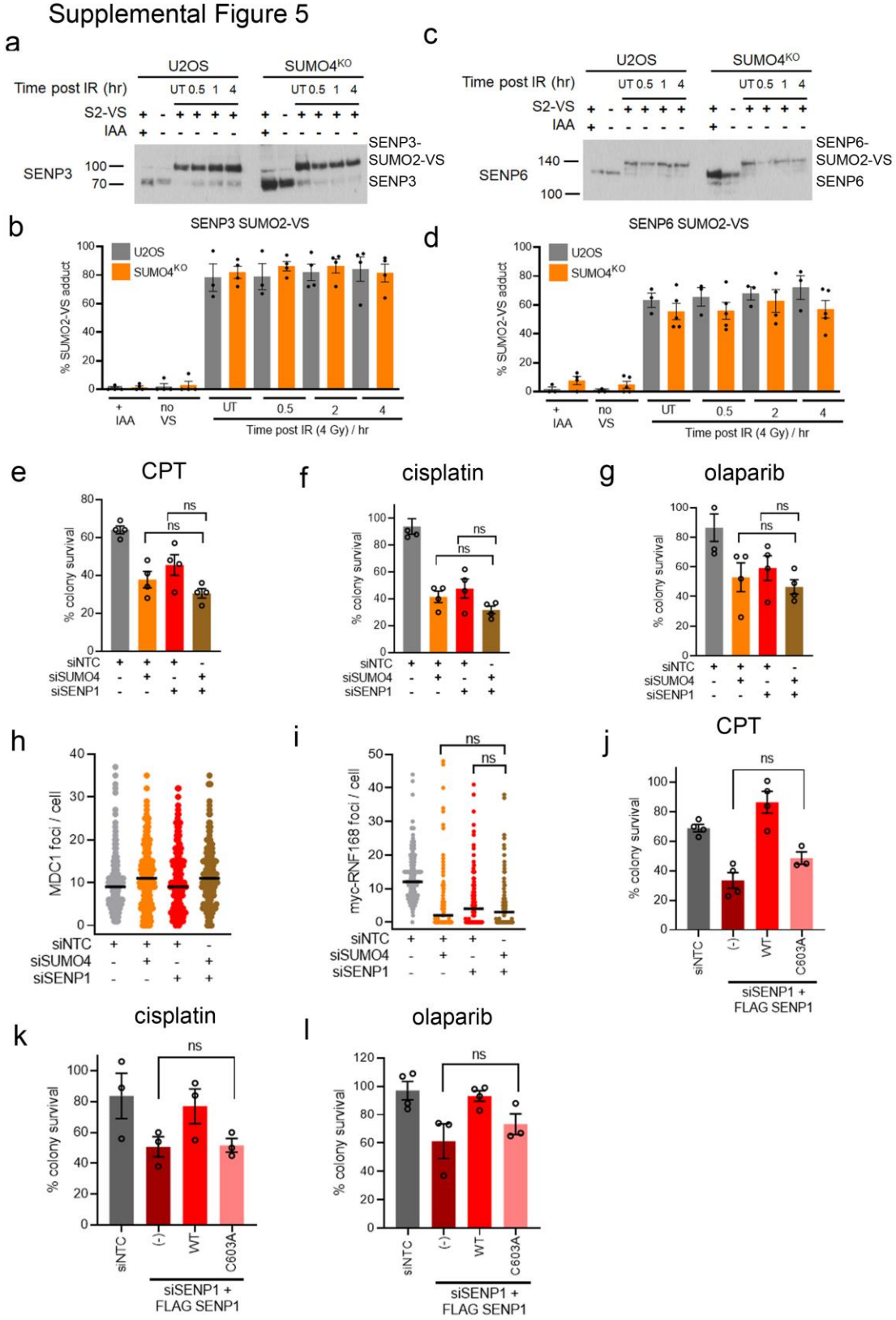

Supplemental Figure 5

a) HA-SUMO2 vinyl sulfone labelling of SENP3 in cell extracts from U2OS or U2OS SUMO4^{KO} that had been either untreated (UT) or irradiated with (4 Gy). Reactions were immunoblotted with SENP3 antibody and the relative amount of upper band (SUMO1-VS labelled SENP3) versus unlabelled SENP3 (lower band) was calculated from 4 experiments. As controls, lysates were incubated with the cysteine protease inhibitor IAA to prevent labelling (+ IAA) or were not incubated with HA-SUMO2 vinyl-sulfone (no S2-VS).

b) Quantification of **a).**

c) as for **a)** but with SENP6 antibody.

d) Quantification of **c).**

e) Colony assays in U2OS treated with siRNA to SENP1, SUMO4 or both for 48 hr prior to CPT (1 μM 2 hr) Error bars = SEM, n=3.

f) as for e) but cisplatin (1 μM 2 hr)

g) as for e) but olaparib (10 μM 2 hr).

h) U2OS siRNA depleted for 48 hr with indicated siRNA before 4 Gy IR and fixing 2 hr later. Cells were immunostained with MDC1 antibody and counted for foci / cell. N= ~150 cells from 3 experiments. Bars show mean.

i) As for h) but using myc-RNF168 expressing U2OS and immunostaining for myc.

j) U2OS or U2OS-FLAG SENP1 were treated with SENP1 siRNA for 48 hr with concomitant dox addition to induce expression of siRNA resistant SENP1 cDNA. Cells were treated with CPT (1 μM 2 hr) prior to plating for colony survival. N=4, error bars show SEM, and statistical significance is determined by two tailed t-test.

k) as for j) but with cisplatin (1 μM 2 hr).

l) as for j) but with olaparib (10 μM 2 hr).